control) or the vehicle (6% DMSO/40 mM Tris–HCl) and 0.6 mM NADPH were added and incubated at 37°C for 30 min under dark condition. The rate of ROS formation as a fluorescent product was measured by a microplate reader (excitation 485 nm; emission 528 nm). These reactions were repeated three times in duplicate. The data was normalized to control values and the control was assigned a value of 100%.

Statistical evaluation

Statistical analyses were performed using statistical software (JMP 4.0.5J; SAS Institute, Inc., NC, USA). The data obtained from in vivo experiments were compared between two corresponding groups by using the Student's *t* test after the one-way ANOVA. Additionally, Dunnett's test was used to isolate the group(s) that differed significantly from the untreated group. The data from the in vitro experiments were also compared using Dunnett's test. A *P* value of less than 0.05 was considered to be statistically significant.

Results

General observations and histopathological findings in the liver

During the experimental period, neither death nor treatment-related clinical signs were observed in any of the groups. However, significant reduction in body weight gain as well as a slight decrease in food consumption was found in the DC and DMN+ DC + PH groups. Macroscopically, all mice of these two groups killed at weeks 13 and 26 showed discoloration of the liver (data not shown).

On histopathological examinations, there were no remarkable changes in the liver of the untreated and DMN groups at weeks 13 and 26. On the other hand, all mice of the DC and DMN + DC + PH groups at weeks 13 and 26 had centrilobular hypertrophy of hepatocytes. Slight and moderate deposition of lipofuscin was observed in the DC and DMN + DC + PH groups, respectively. Other findings included small necrotic foci in both of these groups treated with DC (Fig. 2).

On histochemical stainings for GGT, no GGT-positive reaction on hepatocytes was observed in the untreated group at weeks 13 and 26. In the DMN + PH group, there was no formation of GGT-positive focus at weeks 13 and 26. On the other hand, the DC group at week 26 showed the formation of GGT-positive foci in the liver, although such a reaction at week 13 was detected at only single cell level. The number and area of GGT-positive foci significantly increased only in the DMN + DC + PH group in comparison with that in the untreated or DMN + PH group at week 13. This group showed the highest value of them at week 26, but the value was not significantly different (Fig. 3, Table 1).

mRNA expression in the liver

Findings of the mRNA expression levels of CYP1A1, POR, TXNRD1, SOD1, and OGG1 in the liver are shown in Fig. 4. The expression levels of almost all these mRNAs significantly increased in the DC and DMN + DC + PH groups as compared to the untreated or DMN + PH group, and their highest levels were observed in the DMN + DC + PH group. However, the time-dependent increases of all these genes were not evident in these two groups.

Formation of 8-OHdG in the liver DNA

The data of 8-OHdG are shown in Fig. 5. On HPLC analysis, the levels of 8-OHdG of all groups at week 26 were approximately twice as high as those at week 13, and the time-dependent increasing tendency was found. In the DMN + DC + PH group, the level of 8-OHdG significantly increased in comparison with that of the DMN + PH group and indicated the highest level at weeks 13 and 26. In addition to this group, the DC group also showed significant increases in 8-OHdG as compared to the untreated group at week 26.

Generation of ROS

As shown in Fig. 6, in the presence of H_2O_2 as the positive control, significant increases were found at 0.1 mM of H_2O_2, and the maximum percentage of increase (approximately 120%) was observed at 1 mM in this condition. In the case of DC, a concentration-dependent increase in ROS production was observed, a significant increase being observed at 0.3 mM or greater concentration of DC. At high concentrations of DC (>1 mM), the percentage of increase was higher than that of H_2O_2. On the other hand, the ROS production was depressed to about 40% of the vehicle control (0 mM) because of a high concentration of DMSO.

Discussion

Oxidative stress is believed to be a result of ROS generation occurring in cells due to exogenous factors or cellular metabolism (Grishko et al. 2005). For example, the active oxygen species can be generated by uncoupling of the microsomal monooxygenase reactions. Superoxide anion and H_2O_2 can be formed during P450 turnover. Superoxide can be produced during the autooxidation of the oxycytochrome P450 complex (Kuthan and Ullrich 1982; Sligar et al. 1974). In the

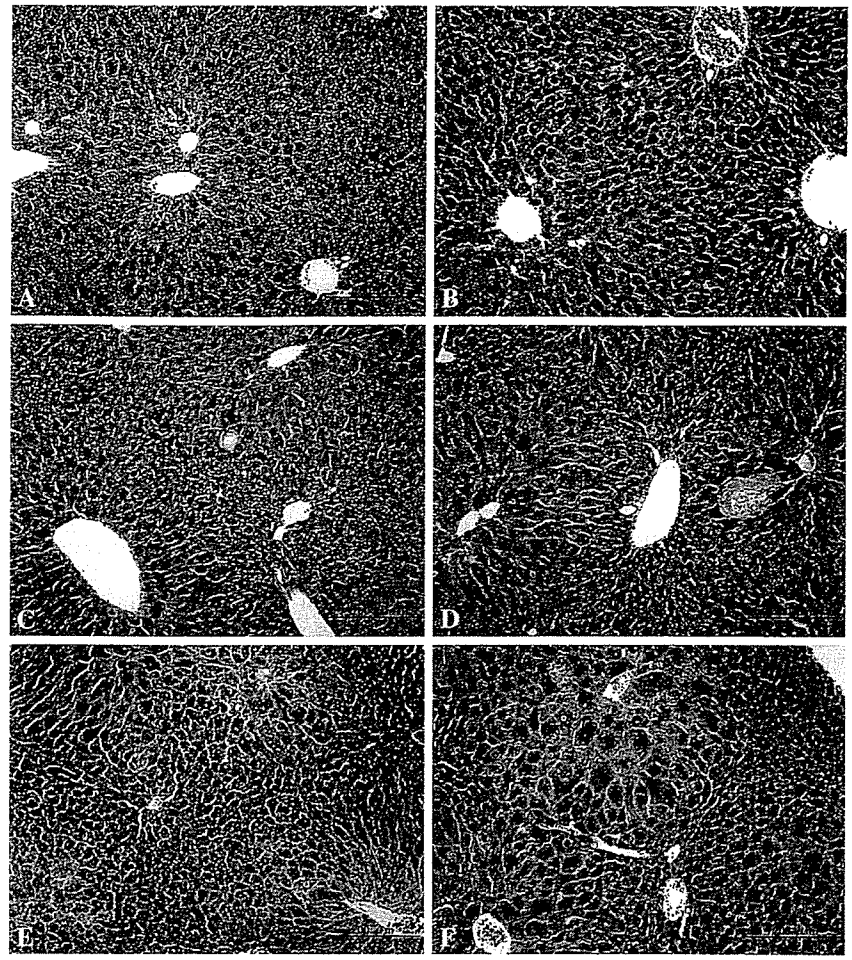

Fig. 2 H–E staining in the liver of hepatectomized mice treated with DC for 13 and 26 weeks after DMN initiation. No remarkable change is observed in the untreated (**a**) and DMN + PH (**b**) group at week 26. Slight centrilobular hypertrophy and some necrotic cells are observed in the DC group at weeks 13 (**c**) and 26 (**d**). Slight to moderate centrilobular hypertrophy and some necrotic cells are observed in the DMN + DC + PH group in weeks 13 (**e**) and 26 (**f**)

present study, the production of ROS in microsomes significantly increased when DC was present at a concentration of 0.3 mM or more in vitro. Although we have no toxicokinetic data such as accurate blood concentrations and systemic distributions of DC achieved by dietary administration in mice, it was previously reported that a single oral administration of 50 mg/kg bw of DC in rats would result in a maximum concentration of 0.1 mM DC (20 μg/ml) in plasma (WHO 2000). The dose level of DC used in the present study is calculated to be equivalent to approximately 150–200 mg/kg bw of DC, and is 3–4 fold higher than that administered to rats in the earlier study. Therefore, it can be expected that since DC was administered to mice by mixing with the diet, the mice are exposed to a limited amount of DC, which is able to produce ROS in hepatocytes for an extended period and approximately for the whole day. Actually, the expressions of mRNAs of metabolism- or oxidative stress-related genes, such as CYP1A1, POR, TXNRD1, and SOD1, in both the DC-treated groups were also significantly up-regulated. These data support our speculation that the oxidative stress was probably induced by ROS generated via the metabolic pathway of DC. However, it is well known that other cellular sources such as mitochondria and peroxisomes also have a potential to generate ROS by various stimulation. Therefore, although measurements of ROS production of these organelles were not performed in our study, it should be considered that the ROS generated in hepatocytes of the DC-treated group are derived from these organelles as well as the metabolic pathway of DC.

Reactive oxygen species can interact with multiple macromolecules, including lipids, nucleic acids, and proteins (Grishko et al. 2005). 8-OHdG, a marker of oxidative DNA damage, is potentially involved in the carcinogenesis in various experimental models, and is known as one of the causes for DNA point mutations such as G–T transversion (Kasai 1997; Nakae et al. 1997; Shibutani et al. 1991). Significant induction and steady elevation of 8-OHdG are considered to play an important role in chemically induced carcinogenesis (Shibutani et al. 1991). In the present study, a significant increase of 8-OHdG level was observed in the DMN + DC + PH and DC alone groups, which showed the formation of GGT-positive foci. These results suggest that the long-term treatment of DC at this dose has the potential to cause oxidative DNA damage. It has been reported that 8-OHdG DNA adducts are repaired by an enzyme OGG1, and the inactivation of OGG1 mRNA in yeast and mice leads to an elevated frequency of spontaneous mutation (Dybdahl et al. 2003; Shinmura and Yokota 2001). In fact, Kinoshita

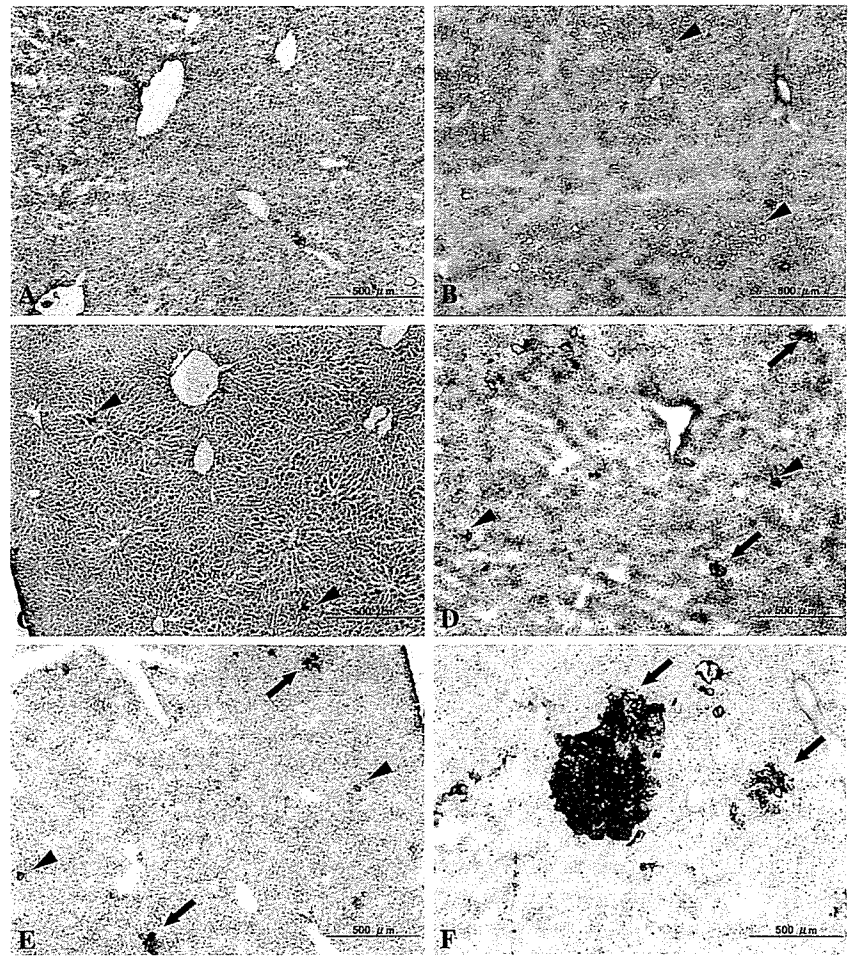

Fig. 3 Histochemical staining of GGT in the liver of hepatectomized mice treated with DC for 13 and 26 weeks after DMN initiation. No positive reaction is observed in the untreated group at week 26 (**a**). GGT-positive reactions at a single cell level (*arrow head*) are detected in the DMN + PH at week 26 (**b**) and the DC group at week 13 (**c**). In addition to GGT-positive cells, the formation of GGT-positive foci (*arrow*) is observed in the DC group at week 26 (**d**). The formation of GGT-positive foci is evident in the DMN + DC + PH group at weeks 13 (**e**) and 26 (**f**)

et al. (2002) reported that the depression of a temporal increase of 8-OHdG induced by a single administration of phenobarbital was due to the reaction following the increase in OGG1. The mRNA expression analyses of the present study showed that the expressions of OGG1 mRNA significantly elevated in both of the groups treated with DC, and the highest level of expression was observed in the DMN + DC + PH group that showed a significant elevation of 8-OHdG. However, a time-dependent remarkable increase of the expression level of OGG1 mRNA was not observed in this group. Therefore, it can be considered that the formation of 8-OHdG in our study was the outcome of the accumulation of imbalance between the DNA repair and DNA damages resulting from the excessive oxidative stress caused by the prolonged DC treatment, although the response of OGG1 mRNA expression was normal.

In many in vivo and in vitro reports on the elevations of 8-OHdG level in mammalian cells exposed to genotoxic or nongenotoxic carcinogens, it is speculated that the formation of 8-OHdG may be one of the causes of point mutations that contribute to the activation of oncogenes or the inactivation of suppressor genes leading to tumorigenesis (Cheng et al. 1992; Kamiya

Table 1 Quantitative data of GGT positive cells and foci in the liver of hepatectomized mice treated with DC for 13 weeks after DMN initiation

Group	Number of animals	GGT positive focus (> 0.05 mm)	
		Number (No./cm^2)	Total area (mm^2/cm^2)
13 weeks			
Untreated	3	0[a]	0
DC	3	0	0
DMN + PH	5	0	0
DMN + DC + PH	5	13.89 ± 11.22*,†	0.072 ± 0.059*,†
26 weeks			
Untreated	7	0	0
DC	7	1.19 ± 3.15	0.004 ± 0.012
DMN + PH	15	0	0
DMN + DC + PH	10	7.32 ± 13.41	0.234 ± 0.640

* Significantly different from the DMN + PH group at $P < 0.05$ (t test)
† Significantly different from the untreated group at $P < 0.05$ (Dunnett's test)
[a]Data are mean ± SD

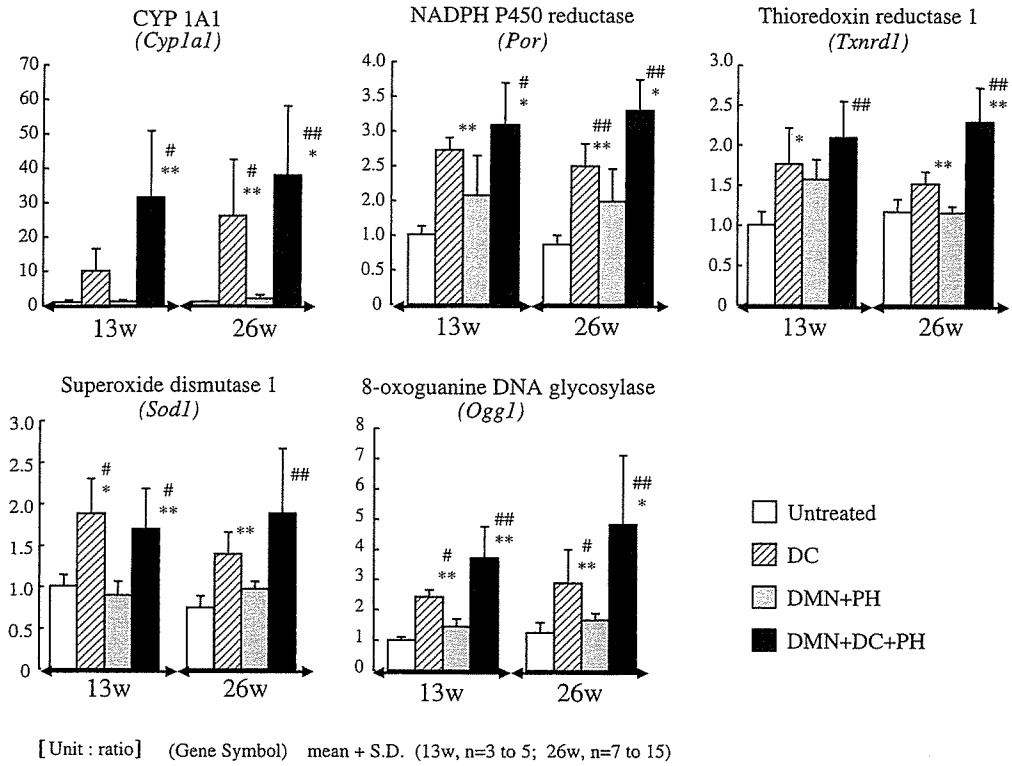

Fig. 4 mRNA expression in the liver of hepatectomized mice treated with DC for 13 and 26 weeks after DMN initiation. *Columns* represent the mean ± SD. * or ** represents the significant difference from the untreated group or DMN + PH group at $P < 0.05$ or 0.01, respectively (*t* test/ ANOVA). # or ## represents the significant difference from the untreated group at $P < 0.05$ or 0.01, respectively (Dunnett's test)

et al. 1992; Umemura et al. 1998). Klaunig et al. (1995, 1998) reported the possibility that subchronic exposure of ROS resulted in the modulation of the expressions of genes such as growth regulatory genes and cell communication genes which are associated with the hepatocarcinogenesis caused by oxidative stress in mice. However, it is unclear whether the gene mutations and modulations that are induced by the treatment with DC or by DNA damages originating from the oxidative stress result in the formation of DC-induced hepatocellular tumors. Recently, *gpt* delta transgenic mice and rats in which it is possible to detect mutations, including point mutations and long deletions of genes in in vivo, have been developed, and many data on carcinogens have been accumulated (Kanki et al. 2005; Masumura et al. 1999; Nishikawa et al. 2001; Nohmi et al. 1996). The study using *gpt* transgenic mice is useful to clarify the location and the amount of mutations that occur when the 8-OHdG formation is detected in the DNA of the liver of DC-treated mice.

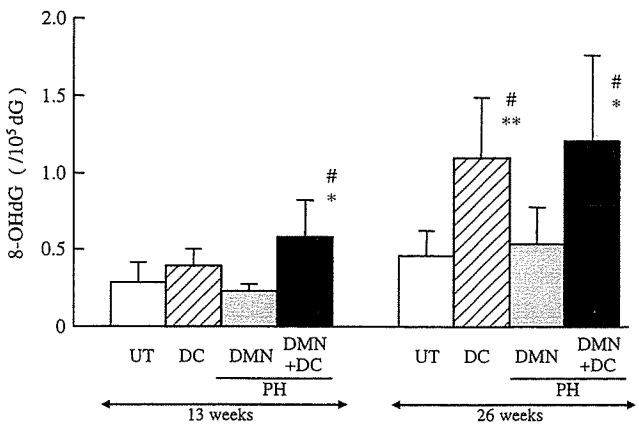

Fig. 5 Levels of 8-OHdG in the liver DNA of hepatectomized mice treated with DC for 13 and 26 weeks after DMN initiation. *Columns* represent mean ± SD. *, ** represents a significant difference from the each control (untreated or DMN + PH) group at $P < 0.05$ or 0.01 (*t* test). # represents a significant difference from the untreated group at $P < 0.05$ (Dunnett's test)

In the present study, during the stage that showed formation of preneoplastic foci, remarkable deposition of lipofuscin was histologically observed in the liver of the DMN + DC + PH group. Lipofuscin is one of the age-associated pigments that have been regarded as cellular debris derived from lipid peroxides formed by oxidative stress, including free radicals (Tsuchida et al. 1987). Therefore, it can be inferred that the increase in the oxidative markers level was induced by oxidative stress, suggesting the high possibility that treatment with DC at 1,500 ppm induces oxidative stress. Furthermore, the formation of GGT-positive foci was observed in the DC alone group at week 26 as well as the DMN + DC + PH group at weeks 13 and 26. In our previous 7-week study with DC, GGT-positive reaction was also observed as a single cell but not as a focus in the DC alone group, while a significant increase of such a focus was found in the liver of mice treated with DC after initiation treatment of DMN (Moto et al. 2005). These findings may suggest that

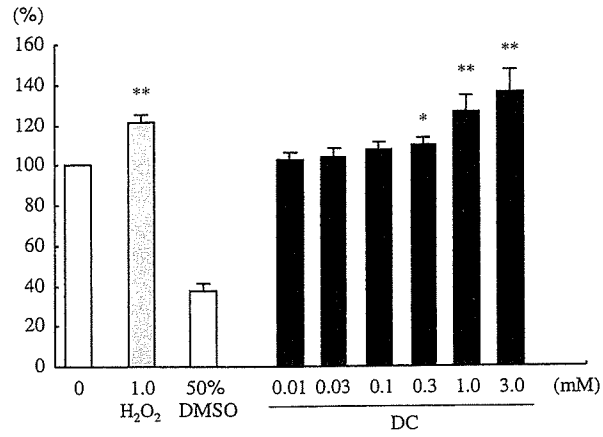

Fig. 6 Effects of DC on hepatic-microsomal ROS production. Microsomes were prepared from the liver of male mice and the formation of DCF as a reactive marker of ROS was measured at excitation 485 nm/emission 528 nm. *Columns* represent the relative value of fluorescent strength estimated at 100% in the absence of DC (0 mM). Values are mean ± SD of three times assays performed in duplicate. * or ** represents significant differences from the vehicle (0 mM) at $P < 0.05$ or 0.01, respectively (Dunnett's test)

cellular altered foci, which are probably derived from gene mutations induced by DNA damages attributable to the oxidative stress, are developed by the treatment of DC. However, the possibility that cellular altered foci originating from spontaneous gene mutations are grown up by the prolonged stimulation of cell proliferation due to the tumor promoting effect of DC cannot be ruled out. Further studies are needed to clarify why such altered foci were induced in the DC alone group by the prolonged treatment of DC for more than 26 weeks.

In conclusion, our data in the present study indicate that DC has potentials to generate ROS via its metabolic pathway and to induce oxidative stress including oxidative DNA damage. These results suggest the possibility that DNA damage originating from the oxidative stress induced by DC results in the induction of hepatocellular tumors in mice, but a long-term treatment with high doses of DC is necessary for the induction of oxidative DNA damage via oxidative stress. In general, it is well recognized that genotoxic carcinogens have direct effects on DNA or chromosomes and there is no threshold on these effects. However, it has been reported that genotoxicity of DC was negative in in vitro studies in the presence and absence of S9 mix (WHO 2000) and a single oral administration of DC did not induce any in vivo DNA damage in the liver of mice (Moto et al. 2003). In addition, the enhancement of hepatocarcinogenesis in a carcinogenicity study using mice was observed in the high dose group (> 500 ppm DC in diet) but not in middle and low dose groups (WHO 2000). Therefore, it can be considered that DC is not a genotoxic carcinogen but a nongenotoxic carcinogen, because there is no evidence suggestive of a direct DNA damage of DC but DNA damage secondary to the oxidative stress induced by DC. However, we have to reconsider the appropriateness of the terminology that such a carcinogen inducing secondary DNA damage is categorized into one of the nongenotoxic carcinogens. Further investigations are now in progress to clarify whether the treatment with DC for a prolonged period results in DNA damage via oxidative stresses and, finally, the induction of hepatocellular tumors in mice.

Acknowledgment We are grateful to Novartis Animal Health Co., Ltd. for supplying dicyclanil. This work was supported in part by a grant-in-aid for the research on safety of veterinary drug residues in food of animal origin from the Ministry of Health, Labor and Welfare of Japan (H16-shokuhin-006).

References

Cater KC, Gandolfi AJ, Sipes IG. (1985) Characterization of dimethylnitrosamine-induced focal nodular lesions in the livers of new born mice. Toxicol Pathol 13:3–9

Cheng KC, Cahill DS, Kasai H, Nishimura S, Loeb LA (1992) 8-Hydroxyguanine, an abundant form of oxidative DNA damage, causes G–T and A–C substitutions. J Biol Chem 267:166–172

Coumoul X, Diry M, Robillot C, Barouki R (2001) Differential regulation of cytochrome P450 1A1 and 1B1 by a combination of dioxin and pesticides in the breast tumor cell line MCF-7. Cancer Res 61:3942–3948

Dumple WC, Yamamoto Y (1995) Small-molecule antioxidants in marine organisms: antioxidant activity of mycosporin-glycine. Comp Biochem Physiol 112B:105–114

Dybdahl M, Risom L, Moller P, Autrup H, Wallin H, Vogel U, Bornholdt J, Daneshvar B, Dragsted LO, Weimann A, Poulsen HE, Loft S, (2003) DNA adduct formation and oxidative stress in colon and liver of Big Blue rats after dietary exposure to diesel particles. Carcinogenesis 24:1759–1766

Fortini P, Pascucci B, Parlanti E, D'Errico M, Simonelli V, Dogliotti E (2003) 8-Oxoguanine DNA damage: at the crossroad of alternative repair pathways. Mutat Res 531:127–139

Grishko VI, Rachel LI, Spitz DR, Wilson GL, LeDoux SP (2005) Contribution of mitochondrial DNA repair to cell resistance from oxidative stress. J Biol Chem 280:8901–8905

Hatanaka N, Yamazak H, Kizu R, Hayakawa K, Aoki Y, Iwanari M, Nakajima M, Yokoi T (2001) Induction of cytochrome P450 1B1 in lung, liver and kidney of rats exposed to diesel exhaust. Carcinogenesis 22:2033–2038

Kamiya H, Miura K, Ishikawa H, Inoue H, Nishimura S, Ohtsuka E (1992) c-Ha-*ras* containing 8-hydroxyguanine at codon 12 induces point mutations at the modified and adjacent positions. Cancer Res 52:3483–3485

Kanki K, Nishikawa A, Masumura K, Umemura T, Imazawa T, Kitamura Y, Nohmi T, Hirose M (2005) *In vivo* mutational analysis of liver DNA in *gpt* delta transgenic rats treated with the hepatocarcinogens *N*-nitrosopyrrolidine, 2-amino-3-methylimidazo[4,5-f]quinoline, and di(2-ethylhexyl)phthalate. Mol Carcinog 42:9–17

Kasai H (1997) Analysis of a form of oxidative DNA damage, 8-hydroxy-2′-deoxyguanosine, as a marker of cellular oxidative stress during carcinogenesis. Mutat Res 387:147–163

Kasai H (2002) Chemistry-based studies on oxidative DNA damage: formation, repair, and mutagenesis. Free Radic Biol Med 33:450–456

Kinoshita A, Wanibuchi H, Imaoka S, Ogawa M, Matsuda C, Morimura K, Funae Y, Fukushima S (2002) Formation of 8-hydroxydeoxyguanosin and cell-cycle arrest in the rat liver via generation of oxidative stress by phenobarbital: association with expression profiles of $p21^{WAF1/Cip1}$, cyclin D1 and Ogg1. Carcinogenesis 23:341–349

Klaunig JE, Xu Y, Bachowski S, Ketcham CA, Isenberg JS, Kolaja KL, Baker TK, Walborg EF Jr, Stevenson DE (1995) Oxidative stress in nongenotoxic carcinogenesis. Toxicol Lett 82–83:683–691

Klaunig JE, Xu Y, Isenberg JS, Bachowski S, Kolaja KL, Jiang J, Stevenson DE, Walborg EF Jr (1998) The role of oxidative stress in chemical carcinogenesis. Environ Health Perspect 106:289–295

Kuthan H, Ullrich V (1982) Oxidase and oxygenase function of the microsomal cytochrome P450 monooxygenase system. Eur J Biochem 126:583–588

LeBel CP, Bondy SC (1990) Sensitive and rapid quantitation of oxygen reactive species formation in rat synaptosomes. Neurochem Int 17:435–440

Masumura K, Matsui K, Yamada M, Horiguchi M, Ishida K, Watanabe M, Ueda O, Suzuki H, Kanke Y, Tindall KR, Wakabayashi K, Sofuni T, Nohmi T (1999) Mutagenicity of 2-amino-1-methyl-6-phenylimidazo [4,5-b]pyridine (PhIP) in the new *gpt* delta transgenic mouse. Cancer Lett 143:241–244

Moto M, Sasaki Y, Okamura M, Fujita M, Kashida Y, Machida N, Mitsumori K (2003) Absence of *in vivo* genotoxicity and liver initiation activity of dicyclanil. J Toxicol Sci 28:173–179

Moto M, Okamura M, Muto T, Kashida Y, Machida N, Mitsumori K (2005) Molecular pathological analysis on the mechanism of liver carcinogenesis in dicyclanil-treated mice. Toxicology 207:419–436

Nakae D, Mizumoto Y, Kobayashi E, Noguchi O, Konishi Y (1995) Improved genomic/nuclear DNA extraction for 8-hydroxydeoxyguanosine analysis of small amounts of rat liver tissue. Cancer Lett 97:233–239

Nakae D, Kobayashi Y, Akai H, Andoh N, Satoh H, Ohashi K, Tsutsumi M, Konishi Y (1997) Involvement of 8-hydroxyguanine formation in the initiation of rat liver carcinogenesis by low dose levels of *N*-nitrosodiethylamine. Cancer Res 57:1281–1287

Nishikawa A, Suzuki T, Masumura K, Furukawa F, Miyauchi M, Nakamura H, Son HY, Nohmi T, Hayashi M, Hirose M (2001) Reporter gene transgenic mice as a tool for analyzing the molecular mechanisms underlying experimental carcinogenesis. J Exp Clin Cancer Res 20:111–115

Nohmi T, Katoh M, Suzuki H, Matsui M, Yamada M, Watanabe M, Suzuki M, Horiya N, Ueda O, Shibuya T, Ikeda H, Sofuni T (1996) A new transgenic mouse mutagenesis test system using Spi$^-$ and 6-thioguanine selections. Environ Mol Mutagen 28:465–470

Santostefano MJ, Richardson VM, Walker NJ, Blanton J, Lindros KO, Lucier GW, Alcasey SK, Birnbaum LS (1999) Dose-dependent localization of TCDD in isolated centrilobular and periportal hepatocytes. Toxicol Sci 52:9–19

Sequeira DJ, Eyer CS, Cawley GF, Nick TG, Backes WL (1992) Ethylbenzene-mediated induction of cytochrome P450 isozymes in male and female rats. Biochem Pharmacol 44:1171–1182

Serron SC, Dwivedi N, Backes WL (2000) Ethylbenzene induces microsomal oxygen free radical generation: antibody-directed characterization of the responsible cytochrome P450 enzymes. Toxicol Appl Pharmacol 164:305–311

Shibutani S, Takeshita M, Grollman AP (1991) Insertion of specific bases during DNA synthesis past the oxidation-damaged base 8-oxodG. Nature 349:431–434

Shimada T, Hayes CL, Yamazaki H, Amin S, Hecht SS, Guengerich FP, Sutter TR (1996) Activation of chemically diverse procarcinogens by human cytochrome P-450 1B1. Cancer Res 56:2979–2984

Shimada T, Inoue K, Suzuki Y, Kawai T, Azuma E, Nakajima T, Shindo M, Kurose K, Sugie A, Yamagishi Y, Fujii-Kuriyama Y, Hashimoto M (2002) Arylhydrocarbon receptor-dependent induction of liver and lung cytochromes P450 1A1, 1A2, and 1B1 by polycyclic aromatic hydrocarbons and polychlorinated biphenyls in genetically engineered C57BL/6J mice. Carcinogenesis 23:1199–1207

Shinmura K, Yokota J (2001) The OGG1 gene encodes a repair enzyme for oxidatively damaged DNA and is involved in human carcinogenesis. Antioxid Redox Signal 3:597–609

Sligar SG, Lipscomb JD, Debrunner PG, Gunsalus IC (1974) Superoxide anion production of cytochrome P450 isozymes in male and female rats. Biochem Pharmacol 44:1171–1182

Szejda P, Parce JW, Seeds MS, Bass DA (1984) Flow cytometric quantitation of oxidative product formation by polymorphonuclear leukocytes during phagocytosis. J Immunol 133:3303–3307

Tsuchida M, Miura T, Aibara K (1987) Lipofuscin and lipofuscin-like substances. Chem Phys Lipids 44:297–325

Tsuda H, Sarma DS, Rajalakshmi S, Zubroff J, Farber E, Batzinger RP, Cha YN, Bueding E (1979) Induction of hepatic neoplastic lesions in mice with a single dose of hycanthone methanesulfonate after partial hepatectomy. Cancer Res 39:4491–4496

Umemura T, Takagi A, Sai K, Hasegawa R, Kurokawa Y (1998) Oxidative DNA damage and cell proliferation in kidneys of male and female rats during 13-weeks exposure to potassium bromate ($KBrO_3$). Arch Toxicol 72:264–269

Van Birgelen AP, Smit EA, Kampen IM, Groeneveld CN, Fase KM, Van der Kolk J, Poiger H, Van den Berg M, Koeman JH, Brouwer A (1995) Subchronic effects of 2,3,7,8-TCDD or PCBs on thyroid hormone metabolism: use in risk assessment. Eur J Pharmacol 293:77–85

Walker NJ, Portier CJ, Lax SF, Crofts FG, Li Y, Lucier GW, Sutter TR (1999) Characterization of the dose–response of CYP1B1, CYP1A1, and CYP1A2 in the liver of female Sprague–Dawley rats following chronic exposure to 2,3,7,8-tetrachlorodibenzo-*p*-dioxin. Toxicol Appl Pathol 154:279–286

WHO (2000) Toxicological evaluation of certain veterinary drug residues in food, fifty-fourth meeting of the Joint FAO/WHO Expert Committee on Food Additives. WHO Food Additive Ser 45:75–89

Yoshida M, Miyajima K, Shiraki K, Ando J, Kudoh K, Nakae D, Takahashi M, Maekawa A (1999) Hepatotoxicity and consequently increased cell proliferation are associated with flumequine hepatocarcinogenesis in mice. Cancer Lett 141:99–107

Toxicologic Pathology, 34:744–751, 2006

ISSN: 0192-6233 print / 1533-1601 online
DOI: 10.1080/01926230600932471

Gene Expression Analysis on the Dicyclanil-Induced Hepatocellular Tumors in Mice

MITSUYOSHI MOTO,[1,2] MIWA OKAMURA,[1,2] MASAKO MUGURUMA,[1] TADASI ITO,[1,2] MEILAN JIN,[1] YOKO KASHIDA,[1] AND KUNITOSHI MITSUMORI[1]

[1]*Laboratory of Veterinary Pathology, Tokyo University of Agriculture and Technology, Fuchu, Tokyo 183-8509, Japan*
[2]*Pathogenetic Veterinary Science, The United Graduate School of Veterinary Sciences, Gifu University, Gifu-shi, Gifu 501-1193, Japan*

ABSTRACT

Our previous studies showed the possibility that oxidative stress, including oxidative DNA damage, is involved in the mechanism of dicyclanil (DC)-induced hepatocarcinogenesis at the preneoplastic stage in mice. In this study, the expression analyses of genes, including oxidative stress-related genes, were performed on the tissues of hepatocellular tumors in a two-stage liver carcinogenesis model in mice. After partial hepatectomy, male ICR mice were injected with *N*-diethylnitrosamine (DEN) and given a diet containing 0 or 1500 ppm of DC for 20 weeks. Histopathological examinations revealed that the incidence of hepatocellular tumors (adenomas and carcinomas) significantly increased in the DEN + DC group. Gene expression analysis on the microdissected liver tissues of the mice in the DEN + DC group showed the highest expression levels of oxidative stress-related genes, such as *Cyp1a1* and *Txnrd1*, in the tumor areas. However, no remarkable up-regulation of *Ogg1*—an oxidative DNA damage repair gene—was observed in the tumor areas, but the expression of *Trail*—an apoptosis-signaling ligand gene—was significantly down-regulated in the tumor tissues. These results suggest the possibility that the inhibition of apoptosis and a failure in the ability to repair oxidative DNA damage occur in the hepatocellular DC-induced tumors in mice.

Keywords. Chemical carcinogenesis; dicyclanil; liver; mouse; non-genotoxic carcinogen.

INTRODUCTION

Dicyclanil (DC)—4,6-diamino-2-cyclopropylamino-pyrimidine-5-carbonitrile—is a pyrimidine-derived insect growth regulator that inhibits the molting and development of insects and is used in the field of veterinary medicine to prevent myiasis (fly strike) in sheep. As a result, minimal amounts of the parent drug and its metabolites are occasionally detected as residues in the edible tissues of sheep, such as the muscle, liver, and fat (WHO, 2000). It has been reported that the incidence of hepatocellular carcinomas was increased in mice that were fed a diet containing 1500 ppm of DC for 18 months, but negative results were obtained from the in vivo and in vitro genotoxicity studies of DC (WHO, 2000). Based on these results, the 54th meeting of the Joint Food and Agriculture Organization (FAO)/World Health Organization (WHO) Expert Committee on Food Additives (JECFA) concluded that DC is a nongenotoxic rodent carcinogen (WHO, 2000).

Recently, to clarify the mechanism of DC-induced hepatocarcinogenesis, we performed 2 experiments—a 2-week feeding study of DC in mice and a short-term study conducted using a 2-stage hepatocarcinogenesis model of mice with partial hepatectomy that were administered DC for 7 weeks. The results of the molecular pathological analysis on the livers of the mice that were fed a diet containing 1500 ppm DC for 2 weeks showed an up-regulation of the expression of several metabolism- and/or oxidative stress-related genes such as cytochrome P450 1A1 and 1A2 (*Cyp1a1* and *Cyp1a2*) as well as thioredoxin reductase 1 (*Txnrd1*). In addition to the genes belonging to the same category, fluctuations in the expression of DNA damage/repair genes, such as 8-oxoguanine DNA glycosylase (*Ogg1*) and growth arrest/DNA-damage-inducible alpha (*Gadd45a*), were observed in the liver of the 2-stage hepatocarcinogenesis model of mice that were administered DC at the same dose (1500 ppm) for 7 weeks after an initiation treatment with *N*-dimethylnitrosamine (Moto et al., 2005).

In our second study, we used a two-stage hepatocarcinogenesis model of mice that were fed a diet containing DC for 13 and 26 weeks. In the liver of these mice, significant increases in the number of altered foci positive for γ-glutamyltranspeptidase (GGT-positive foci)—a predictive marker of preneoplastic foci in mice livers (Carter et al., 1985)—and the content of liver DNA 8-hydroxydeoxyguanosine (8-OHdG)—a representative marker of oxidative DNA damage (Kasai, 1997; Nakae et al., 1997; Umemura et al., 1998; Yoshida et al., 1999; Kinoshita et al., 2002; Dybdahl et al., 2003; Fortini et al., 2003) were observed (Moto et al., 2006). Based on these results, it was suggested that oxidative stress is probably involved in the mechanism of DC-induced hepatocarcinogenesis in mice (Moto et al., 2006). However, these evidences including the observed gene expressions were obtained by examining whole liver tissues at a tumor promoting stage of

Address correspondence to: Mitsuyoshi Moto, Laboratory of Veterinary Pathology, Tokyo University of Agriculture and Technology, 3-5-8 Saiwai-cho, Fuchu-shi, Tokyo 183-8509, Japan; e-mail: m-moto@cc.tuat.ac.jp

ABBREVIATIONS: 8-OHdG, 8-hydroxydeoxyguanosine; CYP, cytochrome P450; DC, dicyclanil; DEN, *N*-diethylnitrosamine; FAO, Food and Agriculture Organization; GGT, γ-glutamyltransferase; Hmox1, heme oxygenase 1; JECFA, Joint FAO/WHO Expert Committee on Food Additives; LCM, laser-capture microdissection; Ogg1, 8-oxoguanine DNA glycosylase; PB, phenobarbital; ROS, reactive oxygen species; TNF, tumor necrosis factor; Trail, TNF-related apoptosis-inducing ligand 10; Txnrd1, thioredoxin reductase 1; WHO, World Health Organization.

hepatocarcinogenesis, and it is unclear how these genes were actually expressed in the hepatocellular tumor tissues.

The aim of this study is to investigate the expression of genes including oxidative stress-related genes in the DC-induced tumor areas in mice. Recently, the laser-capture microdissection (LCM) technique was developed; biochemical or molecular biological analyses in small tissue areas can be performed using this technique (Michael et al. 1996; Suarez-Quian et al., 1999). This technique is a useful tool that enables the collection of only target tissues (areas) under the microscope and prevents contamination with non-target tissues. In this study, by using the LCM technique, histopathological examinations and gene expression analyses were performed on the DC-induced liver tumors obtained from the two-stage hepatocarcinogenesis model of mice with partial hepatectomy.

Materials And Methods

Animals and Chemicals

Four-week-old male ICR mice that were purchased from Japan SLC, Inc. (Hamamatsu, Japan) were maintained on a powdered basal diet (MF; Oriental Yeast, Co., Ltd., Tokyo, Japan) and tap water until they were 5 weeks of age. The mice were housed in polycarbonate cages with paper bedding and were maintained under standard conditions (room temperature, 22°C ± 2°C; relative humidity, 55% ± 5%; light/dark cycle, 12 hr). Animal care and experiments were carried out in accordance with the Guide for Animal Experimentation of the Tokyo University of Agriculture and Technology.

DC (CAS No. 112636-83-6) was kindly provided by Novartis Animal Health Inc. (Basel, Switzerland) for the experiment. *N*-diethylnitrosamine (DEN) was purchased from Nacalai Tesque, Inc. (Kyoto, Japan).

Experimental Design

A two-stage liver carcinogenesis model of mice was employed using the modified protocol of Porta et al. (1987) and Lee et al. (1989) (Figure 1). To initiate hepatocarcinogenesis, an ip injection of DEN at a dose of 30 mg/kg body weight was administered to the animals (day 0). Twelve hours before the DEN injection, a two-third partial hepatectomy was performed on the mice to enhance the regeneration of the liver with DNA damage. One week after the DEN injection, mice were fed a powdered diet containing DC at a concentration of 0 or 1500 ppm for 20 weeks. For liver sampling, after 20 weeks, the survivors were sacrificed by exsanguination from the abdominal aorta under ether anesthesia.

At necropsy, tissue samples were collected from all the remaining lobes of the liver. In the mice with liver tumors, the tissues including tumors were sampled. One-third of these samples were fixed with natural-buffered formalin for the histopathological examinations, and a second one-third was embedded in the OCT compound (Tissue-Tek; Miles Inc., Elkhart, USA) to freeze them for the gene expression analysis of the tumor areas and the staining of GGT. The remaining liver samples were weighed, frozen in liquid nitrogen, and stored at –80°C until subsequent gene expression analyses were performed by using two types of low density cDNA microarrays and real-time reverse transcription (RT) polymerase chain reaction (PCR).

Histology

For light microscopy, formalin-fixed liver tissues were embedded in paraffin, and 4-μm-thick tissue slices were sectioned. Hematoxylin and eosin (H & E) staining for the sections was performed according to routine histopathological methods. Histochemical staining of GGT was performed by using frozen liver slices, as described previously (Moto et al., 2005), in order to determine the presence of preneoplastic foci, altered foci, and neoplasms in the frozen sections.

Preparation of RNA from the Liver

For gene selection in the liver tissues by using microarrays and RT-PCR, total RNA was isolated from approximately 30 mg of the frozen liver tissues of all the animals by using an RNeasy Mini Kit (QIAGEN Inc., CA, USA) according to

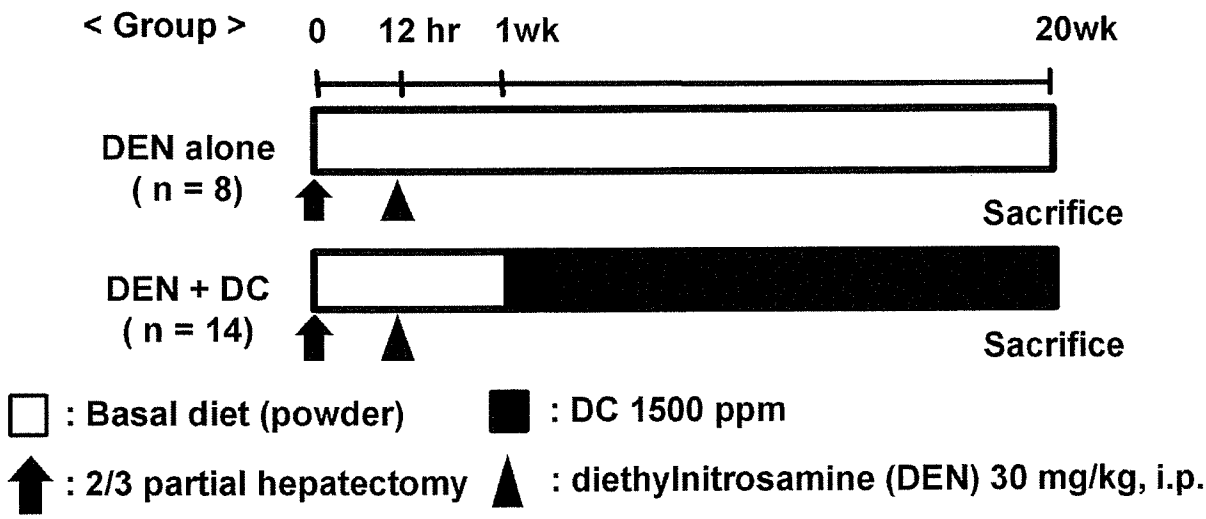

FIGURE 1.—Experimental design.

the manufacturer's instructions. For gene expression analysis in the tumor areas, total RNA was isolated from the livers of three mice in the DEN (nontumor areas) and the DEN + DC groups (tumor and nontumor areas in the same animal), respectively. The frozen tissues embedded in the OTC compound were sliced as 10–15 serial sections with a thickness of 10 μm. One of the frozen sections was used for the histochemical staining of GGT to clarify the area of proliferative lesions. Other sections were stained with 0.05% truidin blue, and the tumor areas (2 carcinomas of 2 mice and 1 adenoma of one mouse) and nontumor areas of 3 mice in the DEN + DC group were collected using the laser microdissection system (AS LMD, Leica Microsystems, Wetzlar, Germany) under light microscopy. LMD samples of each mouse were dissected from 9–14 serial sections and pooled (total >20 mm^2 per each mouse) in RNAlater RNA Stabilization Reagent (QIAGEN Inc., CA, USA). Nontumor areas in 3 mice of the DEN group also collected similarly. The total RNA isolated from the collected samples was treated with DNase and also isolated by the same method described above.

Gene Expression Analyses

The relative expression of genes involved in stress, toxicity, and signal transduction in cancer were analyzed using two kinds of low-density and pathway-specific cDNA microrrays (Stress & Toxicity PathwayFinder cDNA GEArray (MM-12) and the Signal Transduction in Cancer cDNA GEArray (MM-44); SuperArray Inc., Bethesda, MD) containing up to 192 cDNA (96 cDNA per array) fragments from genes associated with these specific biological pathway. Using total RNA from frozen tissues of the 3 mice in which the altered- foci and tumors were respectively observed in the DEN group and the DEN + DC group, cDNA microarrays were performed according to the manufacturer's protocol. Total RNA (3 μg) was reverse transcribed and double-stranded cDNA probes were generated by biotin-16-dUTP incorporation using the AmpoLabeling-LPR Kit (SuperArray), according to the manufacturer's instructions.

Labeled cDNA probes were hybridized overnight. Following repetitive washing, hybridized cDNA probes were detected by chemiluminescence. Membranes were blocked for non-specific binding with GEAblocking solution (SuperArray). Bound biotinylated cDNA probe was detected with alkaline phosphatase-conjugated streptavidin and CDP-Star chemiluminscent substrate (SuperArray). Images of the membranes were recorded on X-ray film and digitally recorded on Bio Imaging System (Lab Works 4.0: UVP Inc., CA, USA). Gene spots were converted into numerical data using ScanAlyze software <http://rana.lbl.gov/EisenSoftware.htm>. Data were further processed with GEArray Analyzer (www.superarray.com), correcting for background noise by subtraction of the minimum value and normalizing to the value of 2 housekeeping genes (ß-actin and GAPDH) of each individual array. Genes were considered present if the expression level was 2 times greater than that of the blank negative control. Genes were considered to be differentially expressed in the DEN + DC group if the mean of fold-changes was less than 0.5 or greater than 2.0 and observed to be statistically significant compared to the DEN group.

Real-time RT-PCR was carried out using the SuperScript III First-Strand Synthesis System (Invitrogen Corp., Carlsbad, CA, USA), and the cDNA aliquots were used in the quantitative real-time RT-PCR with SYBR Green using an ABI Prism 7000 Sequence Detection System (Applied Biosystems, CA, USA). The RT-PCR primers for the genes of *Cyp1a1* (accession No. NM_009992), heme oxygenase 1 (*Hmo1*) (accession No. NM_010442), progesterone receptor (*Pgr*) (accession No.; NM_008829), tumor necrosis factor (TNF)-related apoptosis-inducing ligand 10 (*Trail*) (accession No. NM_009425), *Txnrd1* (accession No. NM_015762), and *Ogg1* (Accession No.; NM_010957) in this study were prepared as reported previously (Moto et al., 2005). To obtain the relative quantitative values for gene expression, β-actin was used as an internal control. Each sample was replicated 3 times, and all reactions were independently repeated 2 times in order to ensure the reproducibility of the results.

Statistical Evaluation

The quantitative data in the DEN and DEN+DC groups were represented as the means ± SD. In gene expression analysis of the liver tissues by real-time RT-PCR, the data were represented as the mean (bar) with individual spots. The significance of the difference in the data of body weight, food consumption, and gene expression ratio between the DEN alone and DEN + DC groups were analyzed by Student's t-test. Data from histopathological examinations were assessed by the Wilcoxon test. A p-value less than 0.05 was considered to be statistically significant. Statistical analyses were performed using a statistical software (JMP 4.0.5J; SAS Institute, Inc., NC, USA).

RESULTS

General Observations and Histopathological Findings in the Liver

During the experimental period, neither death nor remarkable treatment-related clinical signs were observed in either the DEN or the DEN + DC groups. However, a significant reduction in body weight gain was observed in the DEN + DC group at week 3 and from weeks 16 to 20 (Figure 2, Table 1). Macroscopically, the livers of all the mice in the DEN + DC group showed discoloration, and nodules/masses were observed on the surface of the liver in 3 of the 14 mice in this group (Figure 3A).

On histopathological examination, altered hepatocellular foci of the basophilic cell type were observed in both groups,

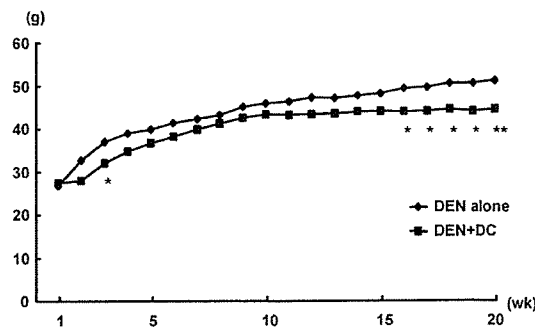

FIGURE 2.—Body weight changes after DC treatment.

TABLE 1.—Body weights, food consumptions, and DC intake in mice treated with DC after DEN initiation.

Group	Number of mice tested	Terminal body weight (g)	Food consumption (g/kg BW/day)	DC intake (g/kg BW/day)
DEN alone	8	51.1 ± 6.8	122.1 ± 16.3	0
DEN + DC	14	44.5**±3.0	119.2 ± 17.3	178.9 ± 25.9

a) Mean ± SD.
**: Significantly different from the DEN group at $p < 0.01$ (Student t-test).

and the incidence of these foci was 43% in the DEN + DC group and 38% in the DEN group. In the DEN + DC group, hepatocellular adenomas (29%) and carcinomas (14%) were also observed, and the total incidence of hepatocellular tumors was 36%; this incidence was significantly higher in this group as compared to the DEN group ($p < 0.01$). In the histochemical staining of GGT performed on frozen sections, altered foci and tumors showed positive reactions (Figure 3,

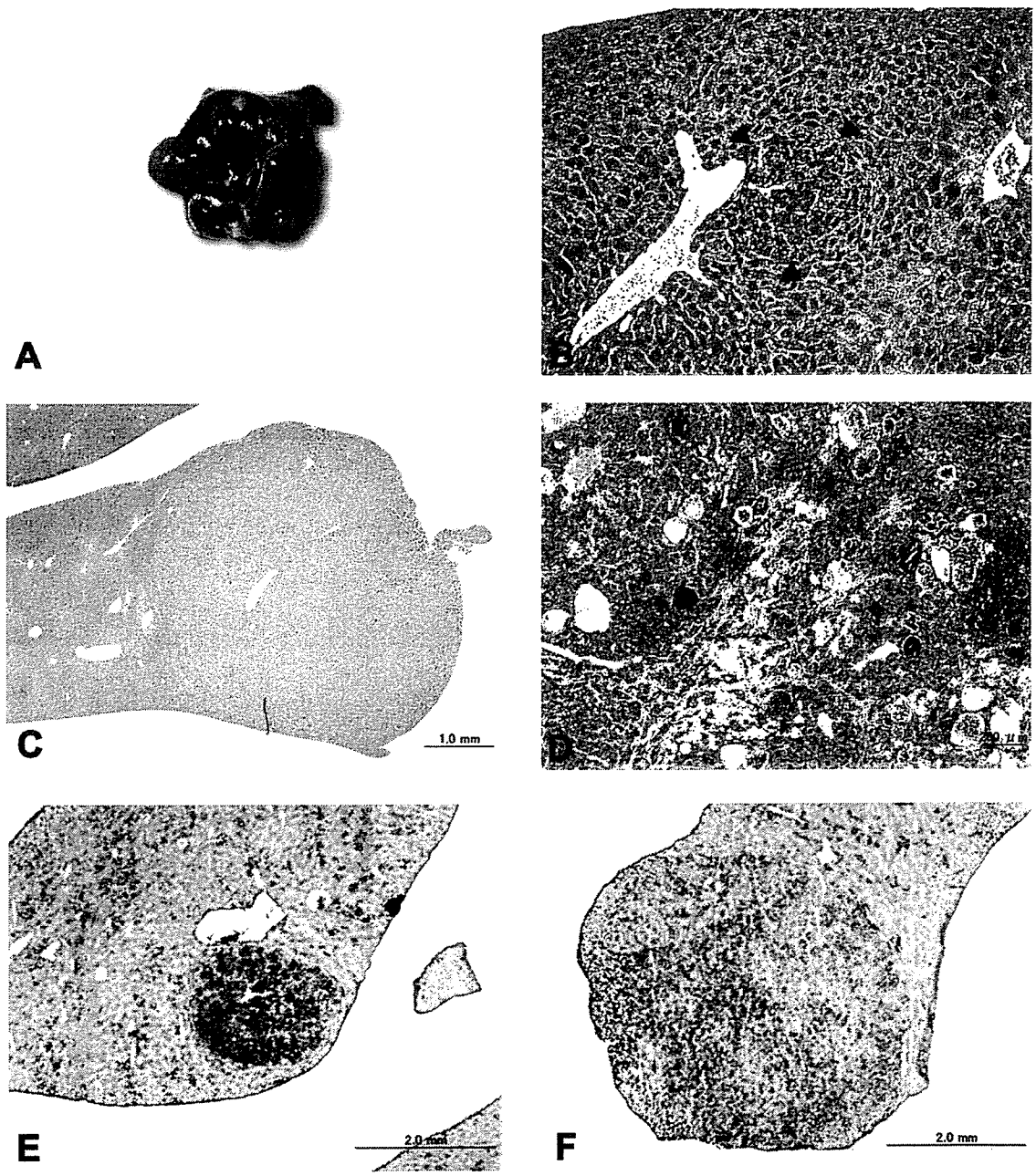

FIGURE 3.—Proliferative lesions in the livers of mice treated with DC after DEN initiation. (A) Macroscopic findings of the liver tumors in mice in the DEN + DC group. (B) Hepatocellular altered focus of a basophilic cell type (enclosed by closed triangles). (C) Hepatocellular carcinoma. Low magnification. (D) Hepatocellular carcinoma that is different from that shown in Figure 3C. Higher magnification. (E and F) Histochemical staining of GGT. GGT-positive reactions are observed in an altered focus (E) and in hepatocellular carcinoma (F).

TABLE 2.—Incidences (percentages) of proliferative lesions in the liver of mice treated with DC after DEN initiation.

Group	Number of mice tested	Altered foci	Adenom	Carcinom	Adenoma + Carcinoma
DEN alone	8	3[a] (38)	0 (0)	0 (0)	0 (0)
DEN + DC	14	6 (43)	4 (29)	2 (14)	5 (36)**

[a] Number of mice.
**: Significantly different from the DEN group at $p < 0.01$ (Wilcoxson test).

Table 2). Similar to other histopathological findings, centrilobular hypertrophy and necrotic foci of the hepatocytes were also observed in the DEN + DC group (data not shown).

Gene Expressions in Liver Tissues

The findings of the gene expressions by the 2 microarray analyses are shown in Table 3. A level of up- or down-regulation greater than 2-fold was observed in 11 genes (up-regulation, 8 genes; down-regulation, 3 genes) of 192 genes in two microarrays. In the stress and toxicity pathway array and the signal transduction array, significant or remarkable up-regulations were observed in the oxidative stress- and metabolism-related genes, such as *Cyp1a1*, *Hmox1*, *Cyp1a2*, and *Pgr* (sex hormone gene), in the DEN + DC group. On the other hand, *Trail* was significantly down-regulated in both arrays.

The validation of gene expression in all animals was performed by real-time RT-PCR for the genes that showed significant and remarkable fluctuations in expression in the microarray analyses (Figure 4). In addition to these genes, *Ogg1* and *Txnrd1*, which we focused on in our previous studies and which are oxidative stress-related genes, were also examined. A significant up-regulation in mean gene expression was observed in *Cyp1a1*, *Hmox1*, *Ogg1*, and *Txnrd1* in the DEN + DC group. In the same group, the mean expression of *Trail* was significantly down-regulated. In the expression analysis carried out on the individual mice in the DEN + DC group, *Trail* showed a tendency toward low levels of expression in the mice with tumors. *Ogg1* also showed a tendency toward low levels of expression in mice with tumors in the DEN + DC group, although its mean expression was significantly up-regulated as compared with its expression in the DEN group. The expression of the other genes in the present examination did not show any remarkable tendency toward either up- or down-regulation in the mice with hepatocellular tumors in the DEN + DC group.

Gene Expression Analysis in the Liver Tumor Areas

In the microarray and real-time RT-PCR analysis, *Ogg1* and *Trail* were selected. In addition to these 2 genes, *Cyp1a1* and *Txnrd1* were also examined as marker genes of oxidative stress. The results of the expressions analysis of these genes in the microdissected tumor areas of the livers of the 3 mice selected from each group are shown in Figure 5.

The mean expression of *Cyp1a1* and *Txnrd1* showed a tendency toward up-regulation in the tumor areas, and a significant up-regulation was observed in the nontumor areas in the mice in the DEN + DC group as compared to the nontumor tissues in the mice in the DEN group. The expression of *Ogg1* was not remarkably up-regulated in the tumor areas, although significant up-regulation was observed in the nontumor areas in the mice in the DEN + DC group. On the other hand, a significant down-regulation of *Trail* was observed in the tumor areas in the mice in the DEN + DC group, although the expression of *Trail* in the nontumor areas in this group was similar to that observed in the DEN group.

DISCUSSION

The histopathological examinations conducted in the present study demonstrated that DC enhanced the induction of hepatocellular tumors in mice, and these data support our previous reports that found that DC has hepatocarcinogenic potential in mice. In the special staining of GGT, the altered hepatocellular foci and tumors in the liver showed a positive

TABLE 3.—cDNA Microarray analysis of the gene expressions in the liver tissues of mice treated with DC after DEN initiation.

Gen Bank Accession No.	Description	Symbol	DEN alone (r = 3) Ratio	DEN alone (r = 3) S.D.	DEN + DC (r = 3) Ratio	DEN + DC (r = 3) S.D.	Classification[a]
	Stress & Toxicity Pathway						
Up							
NM_030677	Glutathione peroxidase 2	*Gpx2*	1.00	0.31	24.09	15.94**	Oxidative and Metabolic stress
NM_009992	Cytochrome P450, family 1, subfamily a, polypeptide 1	*Cyp1a1*	1.00	0.48	16.97	5.48**	Oxidative and Metabolic stress
NM_010442	Heme oxygenase (decycling) 1	*Hmox1*	1.00	0.73	4.14	1.49**	Oxidative and Metabolic stress
NM_010231	Flavin containing monooxygenase 1	*Fmo1*	1.00	0.36	2.85	1.51	Oxidative and Metabolic stress
NM_009993	Cytochrome P450, family 1, subfamily a, polypeptide 2	*Cyp1a2*	1.00	0.32	2.32	0.52*	Oxidative and Metabolic stress
Down							
NM_009425	Tumor necrosis factor (ligand) superfamily, member 10	*Trail*	1.00	0.94	0.04	0.13*	Apoptosis signaling
NM_007836	Growth arrest and DNA (ligand) damage inducible 45 alpha	*Gadd45a*	1.00	0.24	0.48	0.33	Growth arrest and senescence
	Signal Transduction in Cancer						
Up							
NM_007742	Procollagen, type I, alpha 1	*Col1a1*	1.00	0.34	3.14	1.49	MAP kinase pathway
NM_008829	Progesterone receptor	*Pgr*	1.00	0.28	2.94	0.21**	Estrogen pathway
NM_010442	Heme oxygenase (decycling) 1	*Hmox1*	1.00	0.74	2.79	1.72	Hypoxia pathway
NM_009743	RIKEN cDNA A630035D09 gene	*Bcl2l1*	1.00	0.35	2.16	1.11	STAT pathway
Down							
NM_009425	Tumor necrosis factor (ligand) superfamily, member 10	*Trail*	1.00	0.28	0.41	0.03*	PI3/AKT pathway
NM_021283	Interleukin 4	*Il4*	1.00	0.69	0.49	0.12	STAT pathway

[a] Classification is based on the microarray instructions.
'* or **'represent significant differences from the DEN alone group at $p < 0.05$ or 0.01, respectively (t-test).

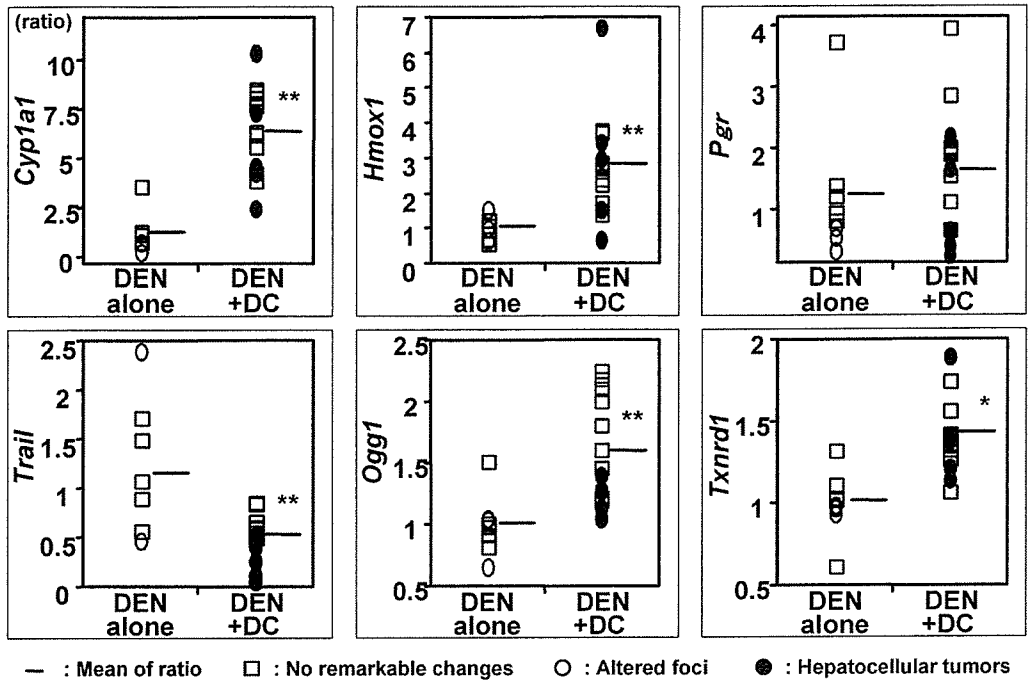

FIGURE 4.—Gene expressions in the livers of mice treated with DC after DEN initiation. Symbols represent each mouse with tumors (closed circles), altered foci (open circles), and no proliferative lesions (squares). Bars represent the mean of each group. "* or**" represent the significant difference from the DEN group at $p < 0.05$ or 0.01, respectively (t-test).

reaction. These data provide supportive evidence indicating that staining of GGT in the liver is a useful tool for the prediction of hepatocellular tumors in mice.

In gene expression analyses carried out by using microarrays in the liver tissues at the tumor formation stage, significant (or remarkable) fluctuations were observed in the expression of certain genes in the DEN + DC group. In addition to the expression of oxidative stress- and metabolism-related genes, such as *Cyp1a1*, *Homx1*, and *Cyp1a2*, significant fluctuations were observed in the expression of *Pgr* and *Trail*. Similar changes in the mean expression of *Cyp1a1*, *Homx1*, and *Trail* in the DEN + DC group were also confirmed by real-time RT-PCR analysis. In our previous study, DC also enhanced the production of reactive oxygen species (ROS) in vitro and the expression of *Cyp1a1* and *Cyp1a2* in the livers of mice at the early stage of hepatocarcinogenesis (Moto et al., 2005, 2006). It has been reported that CYP1A isoforms, such as CYP1A1 and CYP1A2, indirectly result in the production of very large amounts of oxidative stress-inducible substances, such as ROS, in comparison to other CYPs (Puntarulo and Cederbaum, 1998; Canistro et al., 2002). *Hmox1* plays an effective role in counteracting oxidative damage, and it is expected that the activation of this gene has a potential of therapeutic tool for cancer (Fabiana et al., 2004). In addition to these genes, the up-regulation of the mean expression of*Txnrd1* and *Ogg1*, which were focused on as oxidative stress-related genes in our previous studies, were also observed in the DEN + DC group. TXNRD1 plays an important role in the redox regulation of multiple intracellular processes, including DNA synthesis, transcriptional regulation, cell growth, and resistance to cytotoxic agents inducing oxidative stress (Becker et al., 2000; Nyuyen et al., 2005). Based on these results, it can be considered that oxidative stress occurs in the livers of the DC treated-mice at the tumor formation stage, and it is possible that the persistence of oxidative stress plays an important role in hepatocarcinogenesis induced by DC.

In the present gene expression analysis in the liver tissues, tendencies toward low levels of expression were observed for *Ogg1* and *Trail* in mice with hepatocellular tumors in the DEN + DC group. In fact, in the DEN group, the expression of *Ogg1* in the tumor areas was approximately equal to that in the nontumor areas of the DEN alone group; however, the expression level of this gene in the nontumor areas was significantly up-regulated in the DEN + DC group. *Ogg1*, a gene involved in the repair of 8-OHdG, is known as an indicator of oxidative DNA damage and has been shown to be potentially involved in the carcinogenesis in various experimental models (Nakae et al., 1997; Yoshida et al., 1999; Shinmura and Yokota, 2001; Kinoshita et al., 2002, 2003). Our previous study reported that the administration of DC for a period of 13 and 26 weeks increased the formation of 8-OHdG in the liver DNA of mice at the stage of preneoplastic foci formation (Moto et al., 2006). Additionally, *Cyp1a1* and *Txnrd1*, which were used as markers of oxidative stress genes in this study, were remarkably up-regulated in the tumor areas in the livers of mice in the DEN + DC group. Therefore, the present results suggest a possibility that the ability of *Ogg1* to repair the oxidative DNA damage induced by DC failed in the hepatocellular tumors in which high levels of oxidative stress occurred.

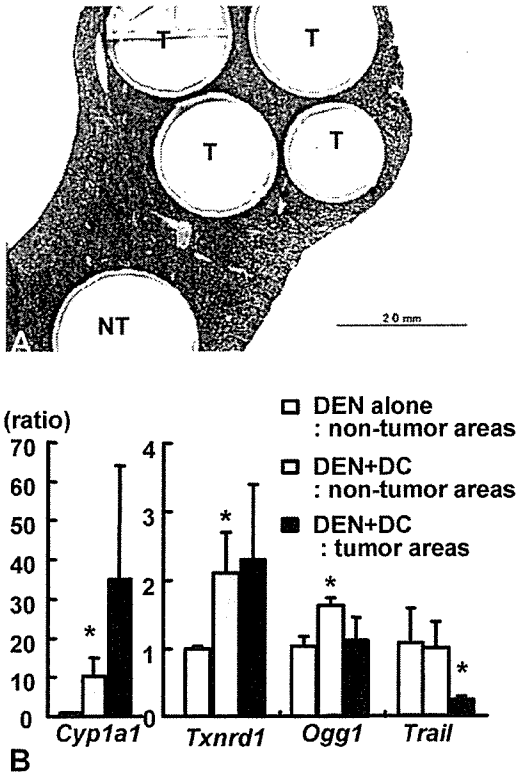

FIGURE 5.—Gene expressions in the hepatocellular tumor areas of mice treated with DC after DEN initiation. (A) Total RNA was purified from the sections microdissected from the tumor areas (T) and non-tumor areas (NT) in the frozen liver slices of the mice. (B) Gene expressions in each area. The tumor areas (closed columns) and nontumor areas (dark columns) in the DEN + DC group were collected from the liver of the same mouse. Columns represent the mean ± SD of the 3 mice. "*" represents significant difference from the DEN group at $p < 0.05$ (t-test).

A significant down-regulation in the expression of *Trail* was observed in the tumor areas in the livers of mice in the DEN + DC group. TRAIL is a member of the TNF family of cytokines that can induce apoptotic cell death in a variety of tumor tissues, and preclinical studies in mice and non-human primates have shown the potential utility of recombinant TRAIL for cancer therapy (Ashkenazi et al., 1999; Walczak et al., 1999; Yagita et al., 2004). Therefore, the down-regulation of *Trail* expression indicates the possibility that apoptosis and the self-regulation of carcinogenesis are inhibited in the tumors induced by DC. It is well recognized that one possible mechanism of nongenotoxic carcinogens is an alteration of apoptosis regulation because dysregulation of apoptosis results in the decreasing ability of cells to undergo apoptosis. For example, phenobarbital (PB) and WY-14643, representative nongenotoxic carcinogens in mice and rats, gradually increase anti-apoptosis proteins during the hepatocarcinogenesis in mice (Christensten et al., 1999). Additionally, it has been reported that short-term treatments of PB showed no increase of apoptosis in the liver of mice (Bursch et al., 2002). In our previous study, the down-regulation of *Trail* expression was not observed in our 2- and 7-week studies of DC. Taking these data into account, it is speculated that *Trail* plays an important role at the later stages of carcinogenesis, such as in the stages of promotion or progression, in the DC-induced hepatocarcinogenicity.

In conclusion, the present investigation on the gene expressions in the hepatocellular tumors induced by DC in a 2-stage hepatocarcinogenesis model of mice have demonstrated the possibility that oxidative stress, failure of the ability to repair oxidative DNA damage, and the inhibition of apoptosis occur in the tumor areas. In addition, the results of our previous and present studies suggest that the continuous treatment of DC induces oxidative stress in the liver and hepatocellular tumors, and oxidative stress plays an important role in the DC-induced hepatocarcinogenesis in mice.

ACKNOWLEDGMENTS

We are grateful to Novartis Animal Health Inc. for supplying DC. This work was supported in part by a grant-in-aid for research on the safety of veterinary drug residues in food of animal origin from the Ministry of Health, Labour and Welfare of Japan (H16-shokuhin-006).

REFERENCES

Ashkenazi, A., Pai, R. C., Fong, S., Leung, S., Lawrence, D. A., Marsters, S. A., Blackie, C., Chang, L., McMurtrey, A. E., Herbert, A., DeForge, L., Koumenis, I. L., Lewis, D., Harris, L., Bussiere, J., Koppen, H., Shahrokh, Z., and Schwall, R. H. (1999). Safety and antitumor activity of recombinant soluble Apo2 ligand. *J Clin Invest* **104**, 155–62.

Becker, K., Gromer, S., Schirmer, R. H., and Muller, S. (2000). Thioredoxin reductase as a pathophysiological factor and drug target. *Eur J Biochem* **267**, 6118–25.

Bursch, W., Wastl, U., Hufnagl, K., and Schulte-Hermann, R. (2002). No increase of apoptosis in regressing mouse liver after withdrawal of growth stimuli or food restriction. *Toxicol Sci* **85**, 507–514.

Canistro, D., Cantelli-Forti, G., Biagi, G. L., and Palini, M. (2002). Re: Dioxin increases reactive oxygen production in mouse liver mitochondria. *Toxicol Appl Pharmacol* **185**, 74–5.

Carter, K. C., Gandolfi, A. J., and Sipes, I. G. (1985). Characterization of dimethylnitrosamine -induced focal nodular lesions in the livers of new born mice. *Toxicol Pathol* **13**, 3–9.

Christensen, J. G., Romach, E. H., Healy, L. N., Gonzales, A. J., Anderson, S. P., Malarkey, D. E., Corton, J. C., Fox ,T. R., Cattley, R. C., and Goldsworthy, T. L. (1999). Altered bcl-2 family expression during non-genotoxic hepatocarcinogenesis in mice. *Carcinogenesis* **20**, 1583–90.

Dybdahl, M., Risom, L., Moller, P., Autrup, H., Wallin, H., Vogel, U., Bornholdt, J., Daneshvar, B., Dragsted, L. O., Weimann, A., Poulsen, H. E., and Loft, S. (2003). DNA adduct formation and oxidative stress in colon and liver of Big Blue rats after dietary exposure to diesel particles. *Carcinogenesis* **24**, 1759–66.

Fabiana, C., Roberto, M., Alejandra G., Alcira B., and Elba, V. (2004). Immunohistochemical analysis of heme oxygenase-1 in preneoplastic and neoplastic lesions during chemical hepatocarcinogenesis. *Int J Exp Pathol* **85**, 213–22.

Fortini, P., Pascucci, B., Parlanti, E., D'Errico, M., Simonelli, V., and Dogliotti, E., (2003). 8-Oxoguanine DNA damage: at the crossroad of alternative repair pathways. *Mutat Res* **531**, 127–39.

Kasai, H. (1997). Analysis of a form of oxidative DNA damage, 8-hydroxy-2′-deoxyguanosine, as a marker of cellular oxidative stress during carcinogenesis.*Mutat Res* **387**, 147–63.

Kinoshita, A., Wanibuchi, H., Imaoka, S., Ogawa, M., Matsuda, C., Morimura, K., Funae, Y., and Fukushima, S. (2002). Formation of 8-hydroxydeoxyguanosin and cell-cycle arrest in the rat liver via generation of oxidative stress by phenobarbital: association with expression profiles of $p21^{WAF1/Cip1}$, cyclin D1 and Ogg1. *Carcinogenesis* **23**, 341–49.

Kinoshita, A., Wanibuchi, H., Morimura, K., Wei, M., Shen, J., Imaoka, S., Funae, Y., and Fukushima, S. (2003). Phenobarbital at low dose exerts hormesis in rat hepatocarcinogenesis by reducing oxidative DNA damage, altering cell proliferation, apoptosis and gene expression. *Carcinogenesis* **24**, 1389–99.

Lee, G. H., Nomura, K., and Kitagawa, T. (1989). Comparative study of diethylnitrosoamine-initiated two-stage hepatocarcinogenesis in C3H, B57BL and BALB mice promoted by various hepatopromoters. *Carcinogenesis* **12**, 2227–30.

Michael, R., Emmert-Buck, R. F., Bonner, P. D., Smith, R. F., Chuaqui, Z., Zhuang, S. R., Goldstein, R. A., and Weiss, L. A. (1996). Laser capture microdissection. *Science* **274**, 998–1001.

Moto, M., Okamura, M., Muto, T., Kashida, Y., Machida, N., and Mitsumori, K. (2005). Molecular pathological analysis on the mechanism of liver carcinogenesis in dicyclanil-treated mice. *Toxicology* **207**, 419–36.

Moto, M., Umemura, T., Okamura, M., Muguruma, M., Ito, T., Jin, M., Kashida, Y., and Mitsumori, K. (2006). Possible involvement of oxidative stress in dicyclanil-induced hepatocarcinogenesis in mice. *Arch Toxicol* **204**, *in press*.

Nakae, D., Kobayashi, Y., Akai, H., Andoh, N., Satoh, H., Ohashi, K., Tsutsumi, M., and Konishi, Y. (1997). Involvement of 8-hydroxyguanine formation in the initiation of rat liver carcinogenesis by low dose levels of *N*-nitrosodiethylamine. *Cancer Res* **57**, 1281–87.

Nguyen, P., Awwad, R. T., Smart, D. D., Spitz, D. R., and Giùs, D. (2006). Thioredoxin reductase as a novel molecular target for cancer therapy. *Cancer Lett* **236**, 164–174.

Porta, G. D., Dragani, T. A., and Manenti, G. (1987). Two-stage liver carcinogenesis in the mouse. *Toxicol Pathol* **15**, 299–34.

Puntarulo, S., and Cederbaum, A. I. (1998). Production of reactive oxygen species by microsomes enriched in specific human cytochrome P450 enzymes. *Free Radic Biol Med* **24**, 1324–30.

Shinmura, K., and Yokota, J. (2001). The OGG1 gene encodes a repair enzyme for oxidatively damaged DNA and is involved in human carcinogenesis. *Antioxid Redox Signal* **3**, 597–609.

Suarez-Quian, C. A., Goldstein, S. R., Pohida, T., Smith, P. D., Peterson, J. I., Wellner, E., Ghany, M., and Bonner, R. F. (1999). Laser capture microdissection of single cells from complex tissues. *Biotechniques*, **26**, 328–35.

Umemura, T., Takagi, A., Sai, K., Hasegawa, R., and Kurokawa, Y. (1998). Oxidative DNA damage and cell proliferation in kidneys of male and female rats during 13-weeks exposure to potassium bromate ($KBrO_3$). *Arch Toxicol* **72**, 264–69.

Walczak, H., Miller, R. E., Ariail, K., Gliniak, B., Griffith, T. S., Kubin, M., Chin, W., Jones, J., Woodward, A., Le, T., Smith, C., Smolak, P., Goodwin, R. G., Rauch, C. T., Schuh, J. C., and Lynch, D. H. (1999). Tumoricidal activity of tumor necrosis factor-related apoptosis-inducing ligand in vivo. *Nat Med* **5**, 157–63.

WHO (2000). Toxicological Evaluation of Certain Veterinary Drug Residues in Food, Fifty-fourth meeting of the Joint FAO/WHO Expert Committee on Food Additives. WHO Food Additive Series 45, pp. 75–89, International Programme on Chemical Safety World Health Organization, Geneva.

Yagita, H., Takeda, K., Hayakwa, Y., Smith, M. J., and Okumura, K. (2004). TRAIL and its receptors as targets for cancer therapy. *Cancer Sci* **95**, 777–83.

Yoshida, M., Miyajima, K., Shiraki, K., Ando, J., Kudoh, K., Nakae, D., Takahashi, M., and Maekawa, A. (1999). Hepatotoxicity and consequently increased cell proliferation are associated with flumequine hepatocarcinogenesis in mice. *Cancer Lett* **141**, 99–107.

Volume 52(7): 903–913, 2004
Journal of Histochemistry & Cytochemistry
http://www.jhc.org

ARTICLE

Microdissected Region-specific Gene Expression Analysis with Methacarn-fixed, Paraffin-embedded Tissues by Real-time RT-PCR

Hironori Takagi, Makoto Shibutani, Natsumi Kato, Haruka Fujita, Kyoung-Youl Lee, Shu Takigami, Kunitoshi Mitsumori, and Masao Hirose

Division of Pathology (HT,MS,NK,HF,K-YL,ST,MH), National Institute of Health Sciences, Tokyo; United Graduate School of Veterinary Sciences (HT,MS,KM), Gifu University, Gifu; and Laboratory of Veterinary Pathology (KM), Tokyo University of Agriculture and Technology, Tokyo, Japan

SUMMARY We have previously shown methacarn to be a versatile fixative for analysis of proteins, DNA, and RNA in paraffin-embedded tissues (PETs). In this study we analyzed its suitability for quantitative mRNA expression analysis of microdissected PET specimens using a real-time RT-PCR technique. Fidelity of expression in the methacarn-fixed PET sections, with reference to dose-dependent induction of cytochrome P450 2B1 in the phenobarbital-treated rat liver, was high in comparison with the unfixed frozen tissue case, even after hematoxylin staining. RNA yield from methacarn-fixed PET sections was equivalent to that in unfixed cryosections and was also not significantly affected by hematoxylin staining. Correlations between the expression levels of target genes and input amounts of extracted RNA in the range of 1–1000 pg were very high (correlation coefficients >0.98), the regression curves being similar to those with unfixed cryosections. Although cell numbers should be optimized for each target gene/tissue, ≥200 cells were necessary for accurate measurement in 10-μm-thick rat liver sections judging from the variation of measured value in small microdissected areas. These results indicate high performance with methacarn, close to that of unfixed tissues, regarding quantitative expression analysis of mRNAs in microdissected PET-specimens. (J Histochem Cytochem 52:903–913, 2004)

KEY WORDS
methacarn
paraffin-embedded tissue
mRNA expression
real-time RT-PCR
microdissection
hematoxylin staining

THE RECENT DEVELOPMENT of microdissection techniques has enabled us to perform biochemical or molecular biological analyses of small tissue areas (Emmert-Buck et al. 1996; Schütze and Lahr 1998). For this purpose, use of cryosections from unfixed frozen tissues has become the gold standard because molecules to be analyzed remain intact. However, preparation of cryosections from unfixed frozen tissue for the purpose of microdissection may not be optimal for routine samples because of the inconvenience in terms of tissue storage and the skill required for preparation and subsequent microdissection. Therefore, tissue embedding after fixation is preferable for microdissected tissue preparations if high yield and quality of molecules can be guaranteed.

For histological assessment, tissue fixation and subsequent paraffin embedding are routinely employed because of the ease of handling tissues and subsequent staining, as well as the good preservation of morphology. Usually, formaldehyde-based fixatives, such as buffered formalin, are used for this purpose. However, with such crosslinking agents there is limited performance in terms of the yield and quality of extracted RNA (reviewed by Srinivasan et al. 2002), protein (Ikeda et al. 1998; Shibutani et al. 2000), and genomic DNA (Srinivasan et al. 2002), with consequent difficulty in the analysis of microdissected, histologically defined tissue areas. Extraction efficiency and quality of molecules are critical for analysis in microdissected cells. Recently, we found that methacarn, a non-crosslinking organic solvent fixative (Puchtler et al. 1970), meets critical criteria for analysis of RNAs, proteins,

Correspondence to: Dr. M. Shibutani, Div. of Pathology, National Institute of Health Sciences, 1-18-1 Kamiyoga, Setagaya-ku, Tokyo 158-8501, Japan. E-mail: shibutan@nihs.go.jp
Received for publication December 3, 2003; accepted March 9, 2004 [DOI: 10.1369/jhc.3A6215.2004].

0022-1554/04/$3.30

and DNAs in microdissected defined areas of paraffin-embedded tissue (PET) sections by simple extraction protocols (Shibutani et al. 2000; Shibutani and Uneyama 2002; Uneyama et al. 2002). With regard to RNA expression analysis using RT-PCR, long RNA fragments as well as rare RNA species can successfully be amplified from methacarn-fixed PET sections (Shibutani et al. 2000).

For RNA expression analysis in microdissected tissue samples, PCR-based techniques are suitable because of their sensitivity with samples having as few as 10 copies of a specific transcript. In this study we examined the suitability of methacarn fixation for measurement of mRNA expression levels in microdissected PET specimens using real-time PCR (Higuchi et al. 1992,1993). For this purpose, we assessed (a) fidelity of mRNA expression in comparison with unfixed frozen tissue, (b) abundance of amplifiable mRNAs in comparison with unfixed cryosections, (c) linearity between the input amount of extracted total RNA and the expression level, (d) effect of tissue staining with hematoxylin, and (e) cell numbers required for practical measurement of mRNA expression in hematoxylin-stained tissue.

Materials and Methods

Animals and Experimental Design

Sprague–Dawley rats from Charles River Japan (Kanagawa, Japan) were used. They were maintained in an air-conditioned animal room (temperature 24 ± 1C; relative humidity 55 ± 5%) with a 12-hr light/dark cycle and allowed ad libitum access to feed and tap water. All animals, including pregnant rats, were housed individually in polycarbonate cages with wood chip bedding.

To measure the dose-dependent induction of cytochrome P450 (CYP) 2B1 mRNA in the liver by treatment with sodium phenobarbital (PB; Wako Pure Chemical Industries, Osaka, Japan), female rats received daily IP injections of PB at doses of 0 (vehicle saline), 1.25, 5, 20, or 80 mg/kg body weight/day for 3 days and were sacrificed 24 hr after the last injection. The highest dose was selected according to the PB-specific enzyme induction protocol described by Kocarek et al. (1998). For practical assessment in microdissected areas, region-specific expression of mRNAs was measured in the hypothalamic medial preoptic area (MPOA) in male and female pups at postnatal day 10, the time point for the late stage of brain sexual differentiation in rats (Rhees et al. 1990a,b).

All animals used in the present study were sacrificed by exsanguination from the abdominal aorta under ether anesthesia. The animal protocols were reviewed and approved by the Animal Care and Use Committee of the National Institute of Health Sciences, Japan.

Tissue Fixation

Methacarn solution consisting of 60% (v/v) absolute methanol, 30% chloroform, and 10% glacial acetic acid was freshly prepared before fixation and stored at 4C until use. At autopsy, livers were removed and 3-mm-thick slices or 5 × 5 × 3 mm-sized tissue blocks were prepared from the left lateral lobe and fixed in methacarn for 2 hr at 4C with gentle agitation. Whole brains of rat pups were also removed and subjected to methacarn fixation. For embedding, liver slices/blocks and coronal brain slices, including the hypothalamus, were dehydrated three times for 1 hr in fresh 99.5% ethanol at 4C, immersed in xylene for 1 hr and then three times for 30 min at room temperature (RT), and immersed in hot paraffin (60C) four times for 1 hr, for a total of 4 hr. Embedded tissues were stored at 4C for up to 6 months until tissue sectioning. Unfixed liver tissue samples, either 3 × 3 × 1 mm or 5 × 5 × 3 mm, were also prepared from portions adjacent to the tissue samples for methacarn fixation and immersed in RNAlater (Ambion; Austin, TX) overnight at 4C, or embedded in Tissue-Tek 4583 OCT compound (Sakura Finetek Japan; Tokyo, Japan) by quick freezing on dry ice. They were stored at −80C until direct extraction of RNA or sectioning before RNA extraction, respectively. For immunohistochemical analysis of MPOA in pups, brains were immersed in 10% neutral buffered formalin (pH 7.4) overnight at RT with gentle agitation. Coronal brain slices that included the hypothalamus were then routinely embedded in paraffin.

Preparation of Tissue Specimens and Microdissection

For assessment of dose-dependent induction of CYP2B1 in the rat liver by PB treatment, methacarn-fixed PETs were sectioned at 10 μm and mounted on 2.5-μm PEN-foil film (Leica Microsystems; Tokyo, Japan) overlaid on a glass slide that had been treated with 3% H_2O_2 for 10 min, rinsed with absolute ethanol, and then dried in an incubator overnight at 37C. The sections were deparaffinized by immersion in xylene twice for 2 min, followed by 99.5% ethanol once for 30 sec. Sections were either unstained or stained with Tissue Tek Hematoxylin 3G (Sakura Finetek Japan) for 10 sec, rinsed briefly with water, and air-dried. For assessment of linearity between the input amounts of total RNA and expression levels of target genes, as well as for estimation of the relative abundance of amplifiable mRNAs, series of 20 10-μm-thick sections were prepared from 5 × 5 × 3-mm unfixed frozen tissues and methacarn-fixed PETs and were collected into 1.5-ml tubes. Integrity of extracted total RNA was also examined in these preparations by judging the resolution of rRNAs in agarose gel. In this experiment, effect of fixation itself on the integrity was also examined with fresh-frozen sections fixed with methacarn for 10 min at 4C. For preparation of tissue sections and hematoxylin staining, RNase-free ultrapure water, prefiltrated with a Gengard filter attached to an Elix 3 ultrapure water system (Millipore; Billerica, MA) was employed. Whole tissue areas of methacarn-fixed PET sections were dissected together with PEN-foil film and collected into 1.5-ml tubes for the dose-dependent expression analysis. With microdissected small tissue areas, hematoxylin-stained 10-μm-thick sections were used and circles of 30-, 50-, and 100-μm radius were microdissected from mid-zonal areas of hepatic lobules using PALM Robot-MicroBeam equipment (Carl Zeiss; Tokyo, Japan). In addition, for assessment of the relationship between the cell number and the amount of extracted total RNA, square ar-

eas of 250 × 250, 500 × 500, and 1000 × 1000 μm were also microdissected.

For microdissection of MPOA, 6-μm-thick sections between pairs of 20-μm-thick sections were prepared from methacarn-fixed rat brain PETs. The 20-μm sections were mounted on PEN-foil film. As shown in Figure 1, localization of the sexually dimorphic nucleus of the preoptic area (SDN-POA), identified as an intensely stained cellular region, was determined under microscopic observation of 6-μm-thick sections stained with hematoxylin and eosin, and the bilateral portions of the MPOA (1000 × 600 μm) containing SDN-POA were microdissected from the adjacent unstained 20-μm-thick sections. Because of sexual dimorphism in the volume of SDN-POA, six to ten sections in males and four to six sections in females were used for microdissection.

RNA Extraction

Quantitative mRNA expression analysis of target genes was performed with a real-time RT-PCR system. In cases of unfixed frozen liver tissue blocks (3 × 3 × 1 mm), whole tissue sections of liver PETs, and microdissected MPOAs from the brain PET sections, total RNA was extracted using RNA STAT-60 (Tel-Test "B"; Friendswood, TX), precipitated with isopropanol in the presence of 2 μg/ml glycogen as a carrier, and reconstituted with 10 μl of ultrapure water treated with diethylpyrocarbonate (Ambion). Unfixed frozen tissue blocks were disintegrated in RNA STAT-60 solution with a Mixer Mill MM300 (QIAGEN; Tokyo, Japan) before extraction. For liver tissue sections of 5 × 5 mm from 5 × 5 × 3-mm unfixed frozen tissues and methacarn-fixed PETs, total RNA was extracted with RNeasy Mini (QIAGEN) according to the manufacturer's protocol, and the final elution volume was set at 30 μl. Contaminating genomic DNA was digested with DNase I (Ambion) at the end of the extraction according to the manufacturer's protocol. One μl of isolated RNA was labeled with a RiboGreen RNA Quantitation kit (Molecular Probes; Eugene, Oregon) and concentrations were estimated with a fluorescence spectrophotometer F2500 (Hitachi; Tokyo, Japan) in 1 ml of total volume with water.

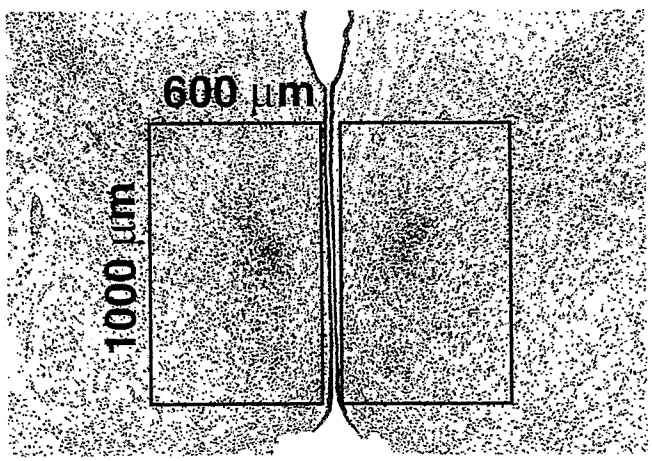

Figure 1 The microdissected area for expression analysis in the MPOA of rat pups at postnatal day 10. The intensely stained cellular regions near the center of each rectangle area are SDN-POAs.

In cases of small tissue areas microdissected from liver PET sections, RNAqueous-Micro (Ambion) was used for total RNA extraction and the final elution volume was set at 20 μl. Contaminating genomic DNA was digested with DNase I included in the kit and the final volume was set to be 25.3 μl.

Real-time RT-PCR

When two-step real-time RT-PCR was planned, RT was performed using 1 μl (200 U) of SuperScript II RNase H⁻ Reverse Transcriptase with 2 μl of 50 μg/ml random hexamers, 1 μl of 10 mM dNTP mix, 2 μl of 10 × PCR buffer, 1.2 μl of 50 mM $MgCl_2$, 2 μl of 0.1 M dithiothreitol, 1 μl of RNase inhibitor, and 9.8 μl of RNA solution in a 20-μl total reaction volume (all reagents were purchased from Invitrogen; Carlsbad, CA). After treatment with 1 μl of RNase H, 1 μl of RT product was subjected to real-time PCR in a 25 μl of total reaction volume with the ABI PRISM 7700 Sequence Detection System (Applied Biosystems Japan; Tokyo, Japan) using either QuantiTect SYBR Green PCR Kit (QIAGEN) or TaqMan Universal PCR Master Mix (Applied Biosystems Japan). With this two-step RT-PCR, mRNA expression levels of CYP2B1, estrogen receptor (ER)α, ERβ, γ-aminobutyric acid transporter type 1 (GAT-1), and glyceraldehyde-3-phosphate dehydrogenase (GAPDH) were measured. Primer Express software (Version 2.0; Applied Biosystems Japan) was used for the design of primer sequences and TaqMan probes. For expression analysis of GAPDH, either SYBR Green or TaqMan probe system was applied. In the latter case, TaqMan Rodent GAPDH Control Reagents (Applied Biosystems Japan) were used. The sequences of primers and probes are listed in Table 1.

With the SYBR Green detection system, mRNA levels of CYP2B1, ERβ, GAT-1, and GAPDH were measured (1 μl of RT product, 12.5 μl of 2 × QuantiTect SYBR Green PCR Master Mix, and 300 nM of primers in a 25-μl total reaction volume). Cycle parameters in this system were as follows: initial activation at 95C for 15 min; 50 cycles of 15 sec at 94C, 30 sec for annealing, and 30 sec at 72C. Annealing temperatures for CYP2B1, ERβ, GAT-1, and GAPDH were 53C, 54C, 54C, and 59C, respectively. With the TaqMan probe detection system, mRNA levels of ERα and GAPDH were measured (1 μl of RT product, 12.5 μl of 2 × TaqMan Universal PCR Master Mix, 900 nM of primers, and 250 nM of TaqMan probe in a 25-μl total reaction volume). Cycle parameters with this system for both genes were: single step of 50C for 2 min, initial activation at 95C for 10 min; 50 cycles of 15 sec at 95C and 60 sec at 60C.

When RT and following real-time PCR were intended to be performed sequentially in one tube, one-step kits, such as the QuantiTect SYBR Green RT-PCR Kit (QIAGEN; for CYP2B1) and the QuantiTect Probe RT-PCR Kit (QIAGEN; for GAPDH) were used with 5 μl of total RNA in a 50-μl total reaction volume according to the manufacturer's protocols. Cycle parameters for CYP2B1 were similar to the above described two-step case, and a RT step at 50C for 30 min was preceded for the initial activation step at 95C for 10 min. In the case of GAPDH, cycle parameters were as follows: single step of 50C for 30 min; single step of 95C for 15 min; and 50 cycles of 94C for 15 sec followed by 60C for 60 sec.

Table 1 Sequences of primers and probes used for real-time RT-PCR

Gene	Accession No.		Sequence	Product size
CYP2B1	M37134	Sense	5′-TTGGCTCCCAAGGACATTG-3′	72 bp
		Antisense	5′-GATCTGGTACGTTGGAGGTATTTTTC-3′	
ERα	Y00102	Sense	5′-GGGCTTCCCCAACACCAT-3′	65 bp
		Antisense	5′-CGTTTCAGGGATTCGCAGAA-3′	
		Probe	5′-TGAGAACTCCCAGGCTCCCCACAA-3′	
ERβ	U57439	Sense	5′-TGCTGGATGGAGGTGCTAATG-3′	82 bp
		Antisense	5′-CGAGGTCGGGAGCGAAA-3′	
GAT-1	NM_024371	Sense	5′-CCTCTGAGATGTTTGGCAAGAA-3′	82 bp
		Antisense	5′-AATTGTACGACCCTTAACGTTGTG-3′	
GAPDH[a]	M17701	Sense	5′-GGCCGAGGGCCCACTA-3′	88 bp
		Antisense	5′-TGTTGAAGTCACAGGAGACAACCT-3′	

[a]For TaqMan PCR, a commercially available TaqMan Rodent GAPDH Control Reagents (Applied Biosystems) was used (sequence information is not available).

As a negative control for RT, reverse transcriptase (−) mock RT samples were included in each PCR experiment.

Immunohistochemical Analysis

Because ERα mRNA is differentially expressed in the MPOA depending on the gender, the corresponding protein expression was also examined immunohistochemically. A series of five 3-μm-thick sections were prepared at 30-μm intervals through the MPOA and the first of each series was stained with hematoxylin and eosin. These sections were examined microscopically and one showing the maximum size of SDN-POA was identified and selected for IHC with ERα in each animal. Deparaffinized and hydrated sections were treated with microwaving for 9 min in 0.01 M citrate buffer (pH 6.0) and treated with 1% periodic acid solution for 10 min. After incubation with mouse anti-ERα monoclonal antibody (Novocastra Laboratories, Newcastle upon Tyne, UK; × 40 dilution), immunodetection was performed using a VECTASTAIN Elite ABC KIT (Vector Laboratories; Burlingame, CA) with a standard protocol using diaminobenzidine as chromogen. The sections were then counterstained with hematoxylin. Digital photomicrographs at a magnification of ×180 were taken with a Fujix Digital Camera system (Fujifilm; Tokyo, Japan), and the numbers of immunostained nuclei within the MPOA (600 × 1000-μm areas) were counted using MacSCOPE (version 2.65; Mitani, Fukui, Japan).

Statistical Analysis

Comparison of data of mRNA expression levels and ERα-immunoreactive cell numbers in MPOA was performed with the Student's *t*-test after confirmation of equal variance of values. Pearson's correlation coefficients were calculated between the input amounts of RNA and the target gene expression levels in the validation studies in the liver and MPOA. Variability was expressed as coefficient of variation (CV).

Results

Integrity of Total RNA

Figure 2 shows the integrity of extracted total RNA from methacarn-fixed PET sections. Judging from the resolution of 18S and 28S rRNAs, integrity of total RNA was well preserved in the methacarn-fixed frozen sections (Figure 2, Lane 2) similar to that from unfixed frozen sections (Figure 2, Lane 1). In the methacarn-fixed PET sections (Figure 2, Lane 3), integrity of both rRNA bands was largely retained, but slight reduction of the band intensity of 28S rRNA was also observed as well as a slight increase of background smearing at the position below the 28S band.

Fidelity of mRNA Expression

Figure 3 shows data for mRNA expression in unfixed frozen tissue and methacarn-fixed PET sections, unstained or stained with hematoxylin. Dose-dependent induction of CYP2B1 mRNA was evident in the livers of rats treated with PB for 3 days. In the unfixed tissue, a clear dose-dependent induction of CYP2B1 was detected, and expression levels relative to that at 80 mg/kg PB were 27.5, 4.95, 1.10, and 0.33%, at 20, 5, 1.25, and 0 mg/kg, respectively. Similar dose-dependent expression was observed in the methacarn-fixed

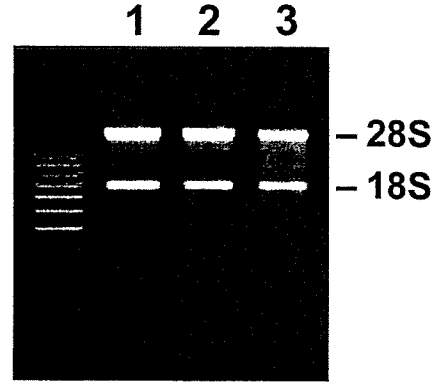

Figure 2 Integrity of total RNA extracted from methacarn-fixed rat liver PET sections. One-μg total RNA samples were resolved in a 1.0% agarose gel and visualized with ethidium bromide. Lane 1, unfixed frozen sections; Lane 2, methacarn-fixed frozen sections; Lane 3, methacarn-fixed PET sections.

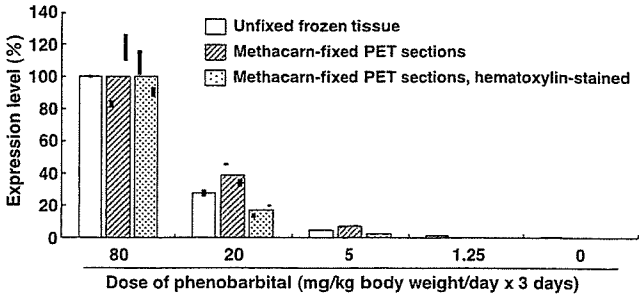

Figure 3 Comparison of gene expression pattern between the unfixed frozen tissue and stained or unstained methacarn-fixed PET sections. For analysis of dose-dependent CYP2B1 expression in the rat liver by PB, one animal was examined at each dose, and therefore the tissue source was set to be identical between preparations at each dose level. In the unfixed frozen tissue, RT was performed with 2 μg of total RNA. For methacarn-fixed PET sections, RT was performed with 335 ng of total RNA. Real-time PCR was performed in duplicate on each RT product. The upper and lower ends of the bars on each column of the graph represent the expression levels measured in duplicate from the same cDNA template.

PET sections irrespective of staining with hematoxylin, although slight suppression was noted at doses of 1.25 and 0 mg/kg. With regard to variability, there was a maximal 47% difference between the values in each RT sample at 80 mg/kg PB (unstained sections). The relative expression levels at 20, 5, 1.25, and 0 mg/kg PB were 38.6, 7.27, 0.21, and 0.06% in unstained sections and 18.1, 2.49, 0.01, and 0.02 in hematoxylin-stained sections, respectively. Reverse transcriptase (−) mock RT samples did not show any amplification on the PCR.

Relative Abundance of Amplifiable mRNA Molecules

To examine the relative abundance of amplifiable mRNA molecules in the methacarn-fixed PET sections, gene expression levels were compared with those in unfixed cryosections using liver of a rat treated with PB at 80 mg/kg body weight/day for 3 days. RNA yields from unfixed cryosections and methacarn-fixed PET sections were determined to be 35.4 ± 11.3, and 42.1 ± 6.0 ng/mm^2 area in 10-μm-thick sections, respectively (n=5). With extracted total RNAs in the range of 1–1000 pg, relative expression of CYP2B1 and GAPDH was determined (Table 2). Although expression signals for both genes could be detected with 1 pg total RNA, values varied when input amount of total RNA was decreased in both tissue section preparations. With 100 and 1000 pg of total RNA, variability of expression data, as judged by the values of CV, was reduced in both unfixed and methacarn-fixed PET sections, with a small reduction of amplifiable mRNAs for both genes in the latter compared with unfixed cryosections (88.2~98.5% for CYP2B1 with statistical difference of $p<0.05$ at 100 pg; 76.5~86.3% for GAPDH with $p<0.05$ at 1000 pg).

Linearity Assessment of mRNA Expression with Input Amount of Total RNA

Figure 4 shows comparisons of regression curves between cryosections and methacarn-fixed PET sections from the liver of a PB-treated rat, based on the data shown in Table 2. In the methacarn-fixed PET sections, the linearity between input amounts of total RNA and expression levels was very high for both CYP2B1 and GAPDH genes and the curves were almost identical with those for unfixed sections. The correlation coefficients in the analysis of CYP2B1 and GAPDH with unfixed frozen sections were 0.997 and 0.990, respectively. Similarly, correlation coefficients in the methacarn-fixed PET sections were 0.991 and 0.982, respectively.

Variability of the mRNA expression data during the processes of RT and after real-time PCR was assessed for four genes with the same RNA sample de-

Table 2 Relative abundance of amplifiable mRNAs in methacarn-fixed PET sections[a]

	No. of samples	Extracted total RNA (pg)			
		1000	100	10	1
CYP2B1					
Unfixed cryosections	5	100.0 ± 7.1[b] (7.1)[c]	8.08 ± 0.41 (5.1)	0.61 ± 0.10 (16.4)	0.12 ± 0.04 (33.3)
Methacarn-fixed PET sections	5	98.5 ± 12.4 (12.6)	7.13 ± 0.69[d] (9.7)	0.64 ± 0.09 (14.1)	0.10 ± 0.04 (40.0)
GAPDH					
Unfixed cryosections	5	100.0 ± 13.3 (13.3)	8.54 ± 0.46 (5.4)	0.79 ± 0.15 (19.0)	0.06 ± 0.04 (66.7)
Methacarn-fixed PET sections	5	76.5 ± 13.6[d] (17.8)	7.37 ± 1.10 (14.9)	0.83 ± 0.37 (44.6)	0.04 ± 0.03 (75.0)

[a]Liver of a rat treated with phenobarbital (80 mg/kg body weight/day IP, once daily for 3 days). One to 1000 pg of total RNA extracted from 10-μm-thick sections by RNeasy Mini was subjected to one-step RT-PCR of GAPDH with the TaqMan probe detection system and CYP2B1 with the SYBR Green detection system.
[b]Relative expression (% of the level at 1000 pg of total RNA from unfixed cryosections). Values are expressed as mean ± SD.
[c]Values in parentheses represent the CV.
[d]Significantly different from the corresponding unfixed frozen section ($p<0.05$ by Student's t-test).

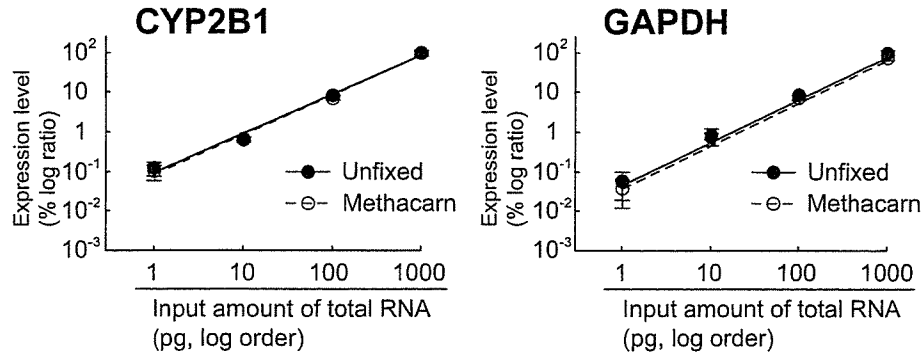

Figure 4 Linearity assessment of mRNA expression in the methacarn-fixed PET sections with the input amount of extracted total RNA in the range of 1–1000 pg. Expression levels of CYP2B1 and GAPDH were analyzed with one-step real-time RT-PCR. Relative expression levels were calculated when the values for the 1000 pg template RNA was accounted as 100% (mean ± SD; n=5). Pearson's correlation coefficients between the input amount of RNA and the expression of CYP2B1 or GAPDH were 0.997 and 0.990 in the unfixed frozen sections, and 0.991 and 0.982 in the methacarn-fixed PET sections.

rived from the MPOA of a male rat on postnatal day 10 (Figure 5). With the total RNA in the range of 5–45 ng, variability in the expression for each gene expressed as CV was mostly within 20%. In addition, high correlation of the expression levels to the input amount of total RNA was observed for all genes examined (0.972, 0.985, 0.965 and 0.985, respectively, for ERα, ERβ, GAT-1, and GAPDH).

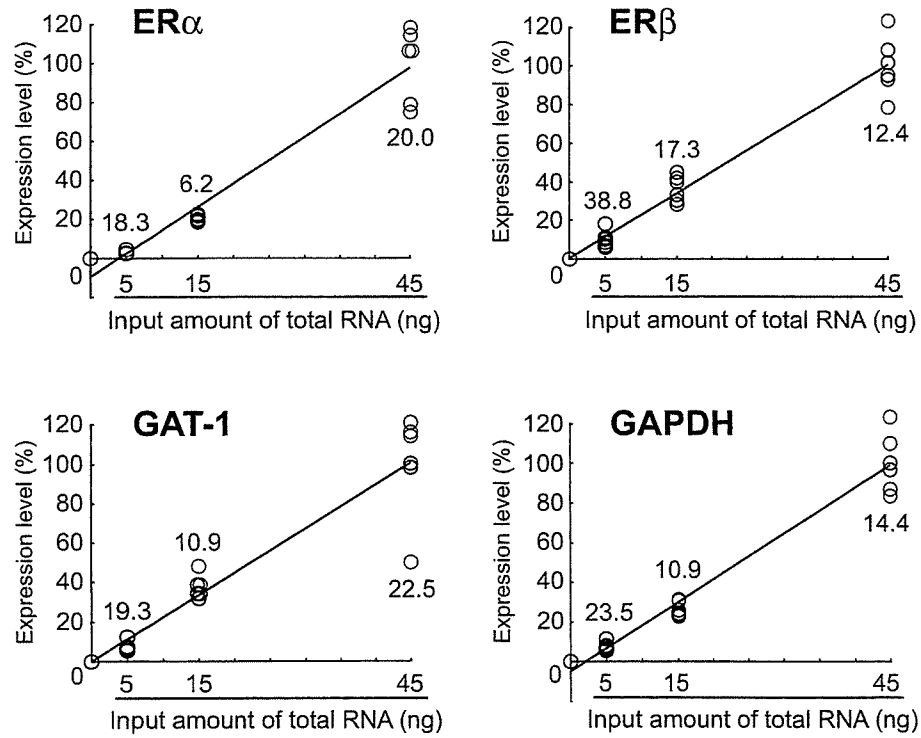

Figure 5 Variability of mRNA expression during the processes of RT and real-time PCR in the microdissected MPOA from methacarn-fixed, paraffin-embedded rat brain tissue. Total RNA extracted from microdissected specimens of MPOA from one male pup was divided to make triplicate samples for each of 5, 15, and 45 ng. RT was performed in a 20 μl of total volume. With 1 μl of RT product in duplicate, real-time PCR was performed for each gene utilizing the TaqMan probe detection system (ERα) or SYBR Green detection system (ERβ, GAT-1, and GAPDH). Relative expression levels were calculated when the values of the 45 ng template RNA was accounted as 100% (n=3). The values in the reverse transcriptase (−) mock RT product using 45 ng total RNA was used as those for zero template. Open circles represent expression levels in each sample. Numerical values in the graphs represent the CV of three samples in duplicate. Pearson's correlation coefficients between the input amount of total RNA and expression level of target gene were 0.972, 0.985, 0.965 and 0.985 for ERα, ERβ, GAT-1 and GAPDH, respectively.